Review



# Comprehensive Analysis of the Potential Toxicity of Magnetic Iron Oxide Nanoparticles for Medical Applications: Cellular Mechanisms and Systemic Effects

Julia Nowak-Jary * and Beata Machnicka

Posted Date: 8 October 2024

doi: 10.20944/preprints202410.0530.v1

Keywords: magnetic nanoparticles; iron oxide nanoparticles; nanotoxicity; oxidative stress; nanomedicine; nanobiotechnology

*Review*

# Comprehensive Analysis of the Potential Toxicity of Magnetic Iron Oxide Nanoparticles for Medical Applications: Cellular Mechanisms and Systemic Effects

**Julia Nowak-Jary and Beata Machnicka**

Department of Biotechnology, Institute of Biological Sciences, University of Zielona Gora, Prof. Z. Szafrana 1, 65-516 Zielona Gora, Poland

* Correspondence: J.Nowak-Jary@wnb.uz.zgora.pl

**Abstract:** Owing to recent advancements in nanotechnology, magnetic iron oxide nanoparticles (MNPs), particularly magnetite ($Fe_3O_4$) and maghemite ($\gamma$-$Fe_2O_3$), are currently widely employed in the field of medicine. These MNPs, characterized by their large specific surface area, potential for diverse functionalization, and magnetic properties, have found application in various medical domains, including tumor imaging (MRI), radiolabelling, internal radiotherapy, hyperthermia, gene therapy, drug delivery, and theranostics. However, ensuring the non-toxicity of MNPs when employed in medical practices is paramount. Thus, ongoing research endeavors are essential to comprehensively understand and address potential toxicological implications associated with their usage. This review aims to present the latest research and findings on assessing the potential toxicity of magnetic nanoparticles. It meticulously delineates the primary mechanisms of MNPs toxicity at the cellular level, encompassing oxidative stress, genotoxic effects, disruption of the cytoskeleton, cell membrane perturbation, alterations in the cell cycle, dysregulation of gene expression, inflammatory response, disturbance in ion homeostasis, and interference with cell migration and mobility. Furthermore, the review expounds upon the potential impact of MNPs on various organs and systems, including the brain and nervous system, heart and circulatory system, liver, spleen, lymph nodes, skin, urinary, and reproductive systems.

**Keywords:** magnetic nanoparticles; iron oxide nanoparticles; nanotoxicity; oxidative stress; nanomedicine; nanobiotechnology

## 1. Introduction

Magnetic iron oxide nanoparticles (MNPs), encompassing magnetite ($Fe_3O_4$) and maghemite ($\gamma$-$Fe_2O_3$), are composed of magnetic domains with permanent magnetization. They represent a unique class of nanostructures extensively utilized in the medical field. Their ferromagnetic properties distinguish them from other nanoparticle types, including polymers, metallic elements (e.g., gold or silver), dendrimers, or carbon tubes. MNPs can be precisely directed to specific locations within the body through the influence of an external magnetic field, rendering them valuable as drug delivery systems, particularly for targeted delivery [1–4]. MNPs have well-established applications, notably in magnetic resonance imaging (MRI) and hyperthermia [5,6]. They are also employed in gene therapy [7], radiolabelling, and internal radiotherapy [8]. Specific iron oxide nanoparticle variants address microbial infections [9,10]. Recent research investigations have increasingly explored the potential of MNPs as valuable tools within the domain of bone tissue engineering [11].

The noteworthy attribute of magnetic nanoparticles for medical applications lies in their capacity for desired activity and biocompatibility within the organism. Biocompatibility is defined as the absence of toxicity, injurious effects, or physiological reactivity about living tissue or systems and the absence of immunological rejection. Well-engineered magnetite and maghemite nanoparticles are considered safe nanostructures, as iron is a naturally occurring trace element in the body. Upon

 doi:10.20944/preprints202410.0530.v1



digestion within lysosomes, the released iron ions can integrate into the natural circulation of this element within the organism. It is posited that the biodegradation mechanism of magnetic nanoparticles bears resemblance to the metabolism of ferritin, a cellular iron storage protein [12,13]. Consequently, several clinically approved iron oxide magnetic nanoparticles are employed in humans as magnetic imaging agents (e.g., GastroMark® and Feridex®), magnetic hyperthermia agents (NanoTherm®), or therapeutic agents for the treatment of iron deficiency (Feraheme®) (El-Boubbou 2018). Nonetheless, the potential toxicity or lack thereof of magnetic nanoparticles is influenced by various factors, including their size, "shell" type, charge, dose, exposure time, and the type of cells or tissues exposed to the nanoparticles. Therefore, comprehensive toxicity studies for each specific type of designed nanoparticles are imperative.

The impact of iron oxide nanoparticles on oxidative stress and their correlation with cell apoptosis is widely acknowledged [14]. The surface coating of the core of magnetic nanoparticles plays a crucial role in mitigating this process [15–18]. Therefore, proper surface functionalization of MNPs not only enhances nanoparticle stability and offers functional groups for the attachment of specific drugs and desired biomolecules but also reduces or eliminates their toxicity within the body [19,20].

This review provides a comprehensive overview of the current understanding of the potential toxicity mechanisms of magnetic nanoparticles at the cellular level and their impact on individual organs and systems.

## 2. The primary mechanisms of toxicity of MNPs at the cellular level

### *2.1. Oxidative Stress*

The internalization of magnetic nanoparticles by cells occurs through phagocytosis or pinocytosis after opsonization, facilitated by specific proteins [21–24]. Opsonization renders MNPs visible to specific cells, allowing them to attach to the cell surface via receptor-ligand interactions. The resulting phagosome or endosome is internalized within the cytoplasm, where it fuses with lysosomes containing enzymes in an acidic environment. Consequently, iron ions are released and can permeate nuclear or mitochondrial membranes, participating in the Haber-Weiss, Fenton, and Fenton-like reactions, which are recognized as primary mechanisms for generating reactive oxygen species (ROS) such as superoxide anions, hydroxyl radicals, and hydrogen peroxide (**Figure 1**) [25]. ROS, in turn, can disrupt membrane structure, impair mitochondrial and other organelle functions, and cause genetic material damage, ultimately initiating cell death pathways [26–28]. Pongrac et al. investigated the levels of intracellular glutathione, mitochondrial membrane potential, cell membrane potential, DNA damage, and the activities of superoxide dismutase (SOD) and glutathione peroxidase (GPx) in murine neural stem cells (NSCs) after exposure to MNPs [29]. It was indicated that the cells had reduced levels of glutathione and impaired activities of SOD and GPx. Additionally, the mitochondria experienced membrane hyperpolarization, disfunction of cell-membrane potential, and DNA damage.

Preprints.org (www.preprints.org) | NOT PEER-REVIEWED | Posted: 8 October 2024 doi:10.20944/preprints202410.0530.v1



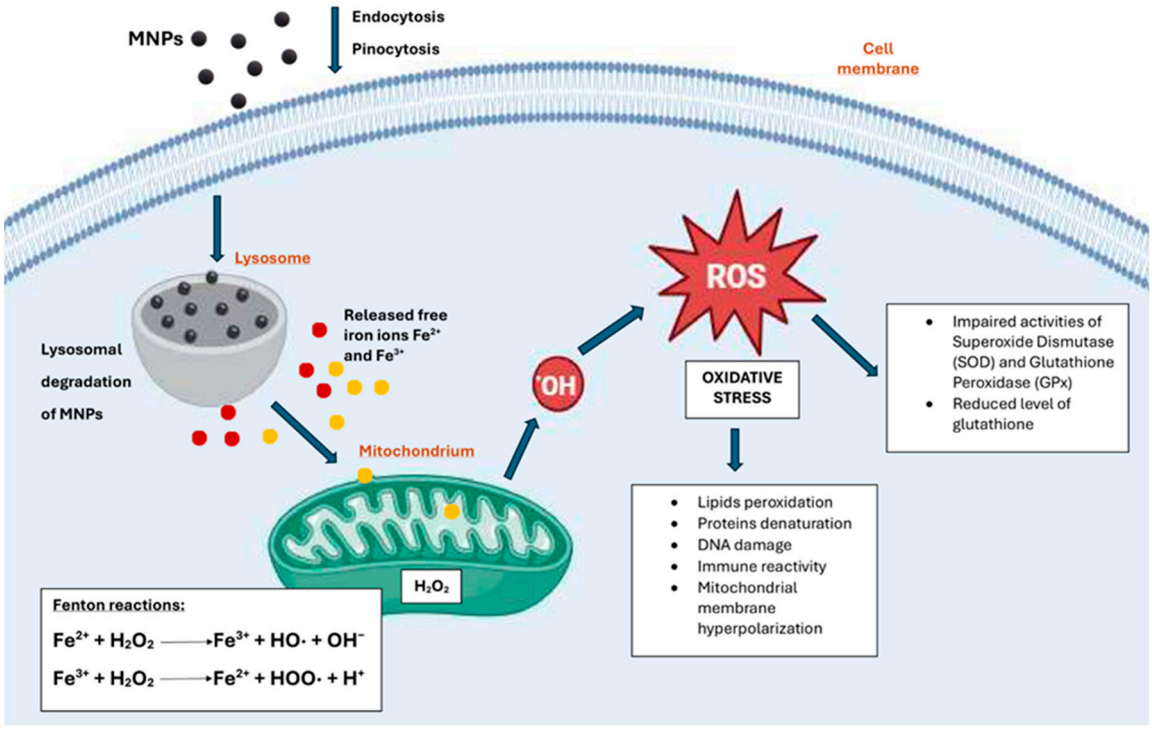


**Figure 1.** Mechanisms of MNPs-mediated oxidative stress. Created with BioRender.com.

Multiple research studies have investigated the generation of reactive radicals ·OH by MNPs. One study by L. Wu et al. reported that MNPs with a diameter below 5 nm exhibited high toxicity towards several organs, particularly the heart, at a dosage of 100 mg/kg [30]. In contrast, nanoparticles with a size above 5 nm did not demonstrate apparent toxicity. In turn, H. Ying et al. found that 30 nm MNPs induced greater free radical production in mouse primary macrophages compared to 10 nm nanoparticles, contradicting the findings of Wu et al [31]. Notably, various cell lines and organs exhibit distinct responses to exposure to iron oxide nanoparticles, indicating different susceptibilities to oxidative stress. Increased generation of ROS due to MNPs exposure has been observed in various cell types, including MCF-7 cells [30], mice primary macrophages [31], rat's lymphocytes [32], human brain-delivered endothelial cells [33], Chinese hamster lung cells [34], osteosarcoma cells [35], brain microglia cells [36], Chinese hamster ovary CHO-K1 cells [37], and human lung A549 cells [38]. Conversely, studies by Hohnholt [39], Lindemann et al. [40], and Remya et al. [41] reported no significant ROS formation after treatment with MNPs.

Applying effective antioxidants is a significant approach to suppressing the generation of reactive oxygen species (ROS). For instance, a recent study highlighted the protective role of oleic acid in mitigating oxidative stress in endothelial cells induced by silica-coated MNPs approximately 19 nm in size [42]. Furthermore, the mitigating effect of ascorbic acid was demonstrated in human hepatocellular carcinoma HepG2 and human lung adenocarcinoma cells [43]. Recent advancements have led to the development of inorganic nanoparticles with antioxidant properties, known as nano-antioxidants [44]. These properties are demonstrated by metal nanoparticles such as silver and gold and transition metal oxides, including copper oxide, nickel oxide, and magnetic iron oxide. The nanoparticles are modified with antioxidants or antioxidant enzymes such as superoxide dismutase, catalase, or oxidase.

The antioxidant properties of nanoparticles are influenced by various factors, including their synthesis method, chemical composition, stability, surface area, size, coating, and charge [45]. Further modification with various phytochemicals has been observed to augment the antioxidant activity of MNPs. Despite the typical generation of free radicals by nanoparticles, their green synthesis enables them to exhibit antioxidant activity [46]. For example, research has shown that magnetic iron oxide nanoparticles synthesized using *Blumea eriantha* demonstrated an antioxidant activity level of 74.94%

 doi:10.20944/preprints202410.0530.v1



[47]. Nevertheless, the mechanisms underlying the antioxidant activity of nanoparticles are not yet fully comprehended and are currently the subject of intensive research [46].

The utilization of magnetic nanoparticles to induce reactive oxygen species (ROS) holds significant promise as a prospective approach in cancer therapy [14]. Elevated levels of free radicals within cells can propagate deleterious effects on cellular components, leading to cellular demise [48,49]. The targeted strategy of cancer treatment necessitates the selective impact of MNPs on cancer cells while preserving the integrity of healthy cells. This targeted effect can be achieved by leveraging the varying ROS generation capacity of MNPs across different cell types. Emerging evidence has underscored the discriminatory action of MNPs in regulating ROS levels in tumor and normal cells. Notably, Ahamed et al. demonstrated the selective induction of apoptosis in cancer cells (HepG2 and A549) through the p53 pathway by MNPs, with no discernible toxicity observed in normal cells [43]. Similarly, Jahanbani et al. reported that MNPs stimulated ROS production and mitigated succinate dehydrogenase activity in complex II of mitochondria isolated from cancerous oral tongue squamous cells while exerting negligible effects on control mitochondria [50]. Furthermore, Shi et al. innovatively developed NanoTrail, wherein the immobilization of Apo2 ligand or tumor necrosis factor (TNF)-related apoptosis-inducing ligand (Apo2L/TRAIL) on MNPs was undertaken to obviate p53-dependent apoptosis within cells [51]. Exploration of this approach revealed an upregulation of the death receptor DR5 by ROS induced via MNPs, leading to amplified TRAIL/Apo2L-based apoptosis and consequential tumor cell death, with minimal adverse impact on healthy organs. In essence, while the instigation of oxidative stress by magnetic nanoparticles may bear unfavorable consequences if it compromises the viability of healthy cells, meticulous design refinements hold the potential to attenuate their cytotoxicity. Conversely, MNPs exhibit the capacity for targeted modulation, selectively obliterating cancerous cells while preserving healthy cells. This unique property bears substantial promise in the advancement of anti-cancer therapeutic modalities.

The mitochondria are the primary site of reactive oxygen species (ROS) production and are particularly susceptible to oxidative stress [52]. Through the induction of oxidative stress, magnetic nanoparticles can result in the impairment and dysfunction of these organelles, leading to alterations in the cell membrane's polarity and the subsequent release of cytochrome C, culminating in apoptosis [53]. Mitochondrial depolarization permits the influx of calcium ions, which subsequently activate the modification and opening of mega-channels (MPTP) located at the inner and outer mitochondrial membrane junction. Comprising voltage-dependent ion channels (VDAC), adenine nucleotide translocase (ANT), and cyclophilin D (CyD), MPTPs undergo modification due to ROS affecting ANT thiol groups. Moreover, pro-apoptotic proteins, Bax and Bak, interact with VDAC, leading to an increase in pore size and the facilitation of cytochrome c release, thereby triggering the caspase 3-dependent apoptosis pathway [54]. Furthermore, free radicals not only impact the oxidation of mitochondrial membranes but also elevate the levels of toxic lipid peroxidation products, including malondialdehyde (MDA) and 4-hydroxy-2-nonenal [55]. Additionally, the presence of ROS leads to mitochondrial DNA damage, disrupting the function of critical mitochondrial enzymes, such as SOD1, SOD2, pyruvate dehydrogenase, aconitase, and L-ketoglutarate dehydrogenase [56]. Elevated levels of free radicals and mtDNA oxidation have been identified in patients with Alzheimer's disease [57]. Moreover, it has been observed that reactive oxygen species bolster the activity of secretase enzymes involved in amyloid production, an aberrant protein associated with Alzheimer's disease. The excessive presence of this protein exacerbates neuronal dysfunction, neurodegeneration, and cognitive impairment in individuals with Alzheimer's disease [58–60]. Additionally, oxidative stress in the mitochondria damages subunits of the mtDNA electron transport chain (ETC), ultimately leading to reduced ATP production.

### *2.2. Genotoxic effects*

The mechanisms of genotoxicity can be classified into two groups: primary genotoxicity (direct or indirect) and secondary genotoxicity, which is associated with inflammatory cells such as macrophages and polymorphonuclear leukocytes [61]. The genotoxic effect of magnetic nanoparticles is primarily attributed to their direct interaction with the DNA in the nucleus (nDNA), leading to

 doi:10.20944/preprints202410.0530.v1



disruptions in genetic material functioning, including interruptions in nDNA chains, nucleotide oxidation, and perturbations in transcription and replication [62,63]. A study by Shahabadi et al. examined the binding of $Fe_3O_4$@$SiO_2$-nicotinamide nanoparticles to calf-thymus DNA (ct-DNA), demonstrating non-covalent interactions such as electrostatic binding, hydrogen bonding, and channel surface binding [64]. This suggests the potential applicability of these nanoparticles in cancer treatment. Conversely, MNPs can indirectly induce genotoxicity through oxidative stress and excessive production of reactive oxygen species, resulting in DNA damage. In the secondary mechanism, activation of phagocytes in the immune response leads to increased oxygen consumption, consequentially releasing $H_2O_2$ due to activation of the NADPH-oxidase system [65].

### *2.3. Cytoskeleton Disruption*

The integrity of the cytoskeleton is vital for cell viability, and any impairment to its structure can lead to cell demise. Actin filaments are primarily responsible for upholding cell architecture and facilitating organelle and vesicle transport. Disruption of these filaments can instigate cell cycle arrest and apoptosis [66]. Instances of cytoskeletal impairment due to oxidative stress have been reported [53], with evidence of non-reactive oxygen species (ROS) mechanisms influencing the action of magnetic nanoparticles on microtubule proteins [67]. Acknowledging the varied cellular sensitivity to MNPs' impact on the cytoskeleton is imperative, analogous to their distinct responses to oxidative stress. This sensitivity diversity holds potential significance in anticancer therapy. For instance, an investigation led by Master et al. examined the effects of 7-8 nm MNPs-polymer complexes on the cytoskeleton of multiple cell lines, including MDA-MB-231 (human triple-negative mammary gland adenocarcinoma), BT474 (human breast ductal carcinoma), and MCF10A (human non-tumorigenic mammary gland cells) [68]. Cells containing internalized magnetic nanoparticles underwent exposure to alternating current (AC) magnetic fields, inducing mechanical disruption of lysosomes, consequently leading to lysosomal membrane permeabilization and subsequent cell death [69,70]. Notably, the investigation revealed that the BT474 cells exhibited increased sensitivity to the treatment compared to the MDA-MB-231 cells, while the healthy MCF10A cells displayed no discernible effect [68].

### *2.4. Cell Membrane Disruption*

All cells are characterized by a membrane electric potential resulting from an ion gradient and selective permeability [71]. Under standard conditions, the ion gradient typically establishes a potential ranging from -10 to -100 mV with a net negative charge on the cytosolic side. Cells possessing a physiological membrane potential are referred to as polarized, while membrane depolarization occurs when the potential is diminished or eliminated. Multiple studies have documented cell membrane depolarization induced by magnetic nanoparticles, leading to alterations in ion channel activity and disruption of cell membrane integrity. For instance, Pongrac et al. observed dose-dependent depolarization of mouse stem cells shortly after exposure to poly(L-lysine)-coated maghemite nanoparticles [72]. In another investigation, two-electrode voltage clamp experiments demonstrated that starch-coated MNPs reduced currents of the Kv1.3 and Kv7.1 potassium channels [73]. Importantly, these direct depolarization effects are specific to particular cell types [74,75].

### *2.5. Changes in the Cell Cycle*

The cellular division process begins with the mitosis (M) phase, comprising the division of cytoplasm and DNA, forming two distinct cells. This is succeeded by the G1 phase, characterized by cellular expansion, organelle duplication, and RNA, proteins, and enzymes synthesis. Subsequently, the S phase involves complete replication of the cell's DNA, and the G2 phase is marked by the cell's preparatory activities for mitosis, including the production of specialized proteins and RNA. Following the G1 phase, a cell may enter the G0 phase, a resting phase, rather than advancing to the DNA synthesis stage (S). Studies suggest that magnetic nanoparticles have the potential to induce

 doi:10.20944/preprints202410.0530.v1



alterations in the cell cycle. For instance, Shokrollahi et al. observed that exposure to $Fe_3O_4$@Glu-Coumarin MNPs prevented HepG2 cells from progressing through the G1 checkpoint, resulting in cell death by apoptosis [76]. MNPs were also found to cause cell cycle arrest in human umbilical vein endothelial cells (HUVECs) [77]. Furthermore, MNPs loaded with doxorubicin (DOX) were shown to restrict the G2 phase in breast cancer (MCF7) cells [78]. Importantly, bare MNPs did not induce any alteration in the G2 phase compared to the control. Tamoxifen-loaded L-lysine-coated MNPs induced cell cycle arrest at the G0/G1 phase in MCF7 cells [79]. Moreover, Majeed et al. reported that engineered green iron oxide nanoparticles with l-arginine exhibited significant toxicity towards breast cancer (MDA-MB-231) cells, leading to cell cycle arrest at the G2/M phase and consequential DNA damage while causing minimal harm to normal cells [80].

### *2.6. Dysregulation of Gene Expression*

In most cases, oxidative stress is found to have a limited impact on the induction of genotoxicity by surface-modified MNPs [81]. Nonetheless, scientific studies indicate that magnetic nanoparticles can directly cause primary DNA damage and disrupt gene expression profiles [62,63,82]. For example, research illustrates that MNPs that are functionalized with glucose and conjugated with Coumarin ($Fe_3O_4$@Glu-Coumarin MNPs) stimulate the expression of *CASP-8*, *p53*, and *MAPK-1* genes while inhibiting the *CASP-9* and *mTOR-1* genes in liver cancer cells [76]. It is important to note that caspases coded by *CASP* comprise a group of cysteine proteases central to apoptotic responses [83]. The initiation of apoptosis is triggered by the activation of Caspase 8. Hence, the overexpression of the *CASP-8* gene led to apoptosis. The *p53* gene acts as a tumor suppressor in human cells, playing a crucial role in cell cycle regulation and initiating cell apoptosis [84]. Consequently, the elevated expression of the *p53* gene in liver cancer cells due to magnetic nanoparticles resulted in anti-proliferative effects. Conversely, *mTOR-1* primarily regulates cell growth and metabolism. Therefore, Shokrollahi et al. have concluded that $Fe_3O_4$@Glu-Coumarin MNPs can effectively inhibit the activation of mTOR-1 signaling pathways, thereby impeding the proliferation and progression of cancer cells [76]. Additionally, Siddiqui et al. have observed significant DNA damage in human umbilical vein endothelial cells (HUVECs) caused by MNPs [77]. Furthermore, exposure to MNPs at concentrations of 100 μg/mL led to the upregulation of proapoptotic genes such as *p53*, *bax*, and *CASP-3* and the downregulation of the antiapoptotic gene *bcl-2* in HUVECs.

### *2.7. Inflammatory Response*

When considering the application of magnetic nanoparticles for medical purposes, it is crucial to evaluate their potential influence on essential innate immune responses. Numerous studies have delved into this subject. For instance, Grosse et al. examined the effects of MNPs coated with organic layers comprising a monolayer of oleic acid and a monolayer of amphiphilic polymer on primary human monocytes in the presence and absence of the Toll-like receptor 4 (TLR4) agonist lipopolysaccharide (LPS) [85]. TLR4 is a receptor that serves as a sensor for lipopolysaccharide (LPS), and its activation leads to the production of several pro-inflammatory, antiviral, and anti-bacterial cytokines [86]. The researchers observed that the tested MNPs did not influence the production of proinflammatory cytokines such as tumor necrosis factor-$\alpha$, interleukin-6, and interleukin-1$\beta$. However, they noted suppression of LPS-induced nuclear factor kappa B activation and the production of proinflammatory cytokines in a dose-dependent manner. In another study, the thromboinflammatory response of uncoated MNPs with a size of 10-30 nm was investigated in whole blood in interaction with endothelial cells [87]. The MNPs were found to elicit a potent thromboinflammatory response, as evidenced by a significantly increased release of 21 out of 27 analyzed cytokines. Furthermore, MNPs significantly increased activation markers of endothelial cells, P/E-selectin, monocytes, granulocytes, and platelets. The experiments also demonstrated cytotoxic effects, as evidenced by elevated levels of lactate dehydrogenase (LDH) and heme. In a related study, Chauhan et al. investigated the potential application of vitamin $K_3$-loaded magnetic nanoparticle-mediated synergistic magneto-thermodynamic therapy (MTD) for cancer treatment [88]. The results indicated that the examined MNPs not only induced the generation

 doi:10.20944/preprints202410.0530.v1



of reactive oxygen species (ROS) but also led to increased expression levels of heat shock proteins and proinflammatory cytokines (IL-6, TNF-$\alpha$, IL-1$\alpha$, IL-1$\beta$).

### *2.8. Disturbance in Iron Homeostasis*

The degradation of MNPs within lysosomes results in the release of iron ions, which subsequently become integrated into the body's natural iron circulation. Free iron is then sequestered as ferritin, a protein that binds with $Fe^{3+}$ ions and stores them in the liver [12,13]. Another protein, transferrin, regulates the concentration of iron ions in the blood plasma and transports them to the tissues. Exceeding the iron storage capacity of these proteins leads to iron overload, disrupting iron homeostasis. Iron overload is defined by elevated ferritin levels (>300 ng/L) and heightened transferrin saturation (>40%) [89]. The excess iron is released into the plasma and circulates in an unbound, redox-active form, causing cellular damage and culminating in organ failure in advanced stages [90,91].

### *2.9. Disturbance of Cell Migration and Mobility*

Alterations in gene regulation and damage to the cytoskeleton can disrupt cell migration [92]. This phenomenon has been observed in endothelial and endothelial progenitor cells [93,94], neural stem cells [95], and macrophages [96]. According to Mohsin et al., the cellular uptake of MNPs markedly increased cell mobility and contraction due to the high levels of intracellular nanoparticles, leading to increased intracellular tension and regulation of cell behavior [97].

The main mechanisms of MNPs toxicity at the cellular level are depicted in Figure 2.

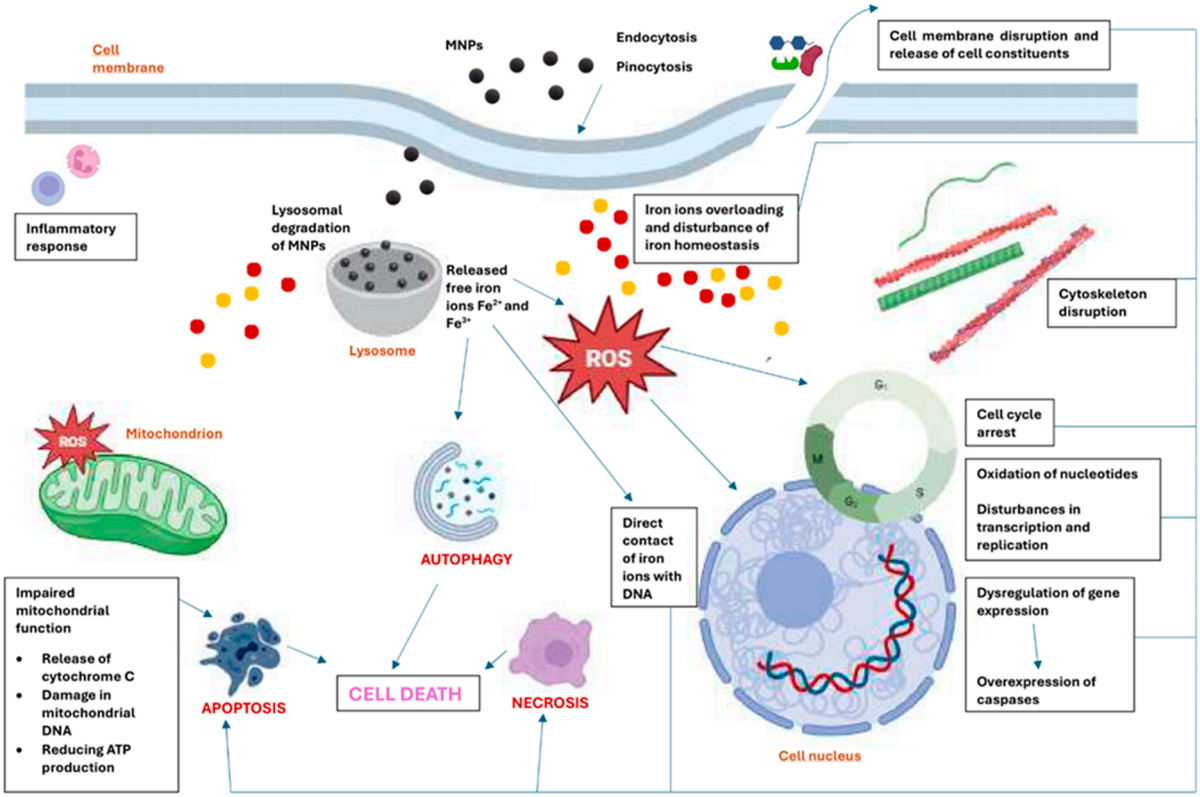


**Figure 2.** Mechanisms of MNPs-mediated toxicity at the cellular level. Created with BioRender.com.

## 3. Systemic and Organ-Toxic Effects of MNPs

### *3.1. Brain and Nervous System*

The blood-brain barrier (BBB) and the blood-cerebrospinal fluid (CSF) barrier act as pivotal defense mechanisms; regulating the passage of substances from the blood into neurons. Their selective permeability restricts the entry of various compounds; allowing only essential substances

 doi:10.20944/preprints202410.0530.v1



such as glucose and amino acids to support the optimal functioning of the nervous system. Studies have demonstrated the potential for magnetic iron oxide nanoparticles to traverse the BBB; dependent on their physicochemical and surface properties. However; accurately predicting whether specific nanoparticles can effectively penetrate neurons remains a significant challenge [98]. *In vitro* studies on the penetration of the BBB by MNPs under a static magnetic field are primarily conducted by administering nanoparticles of various sizes and characteristics to *in vitro* BBB models created through the co-culturing of endothelial cells and astrocytes [99]. One study used brain capillary endothelial cells (BCECs) that were incubated with MNPs at various concentrations (35; 70; and 140 μg/mL) for 24 hours [100]. The study findings revealed that both internalization and transcellular transport processes occurred in the absence of magnetic fields without inducing any toxic effects. Consequently; the authors concluded that the MNPs did not disrupt the barrier's integrity; did not affect cell viability; and were successfully internalized by astrocytes. Recently; Shin and Lee conducted a detailed study on the effects of silica-coated magnetic nanoparticles containing rhodamine B isothiocyanate dye (MNPs@$SiO_2$(RITC)) on BV2 murine microglial cells [101]. Additionally; the authors examined amyloid beta (Aβ) accumulation and molecular changes using integrated transcriptomics; proteomics; and metabolomics (triple-omics) analyses. Following the administration of 0.1 μg/μl MNPs@SiO2(RITC); a significant increase in the amount of Aβ was observed. This discovery points to a notable association between nanotoxicity and Aβ accumulation. Furthermore; the MNPs@$SiO_2$(RITC)-treated BV2 cells displayed evidence of lysosomal swelling; a reduction in proteolytic activity dependent on dosage; and an elevation in lysosomal swelling- and autophagy-related protein levels. Additionally; a decrease in proteasome activity was observed in the BV2 cells following treatment with MNPs@SiO2(RITC); leading to a subsequent reduction in intracellular adenosine triphosphate (ATP)

In the context of neurotoxicity research, *in vivo* studies were undertaken to investigate the impact of MNPs, with specific experiments being conducted using Wistar rats [102]. The animals were administered intravenously by green, carob leaf-synthesized, negatively charged MNPs with a hydrodynamic diameter of approximately 80 nm. The study showed that MNPs had the most significant impact on the hippocampus and striatum of the brain, leading to moderate neuronal degeneration. Additionally, mild neuronal degeneration in the cerebral cortex and slight degeneration in the cerebral cortex were observed. In a separate study, four different types of nanoparticles were administered to Sprague-Dawley rats: dimercaptosuccinic acid (DMSA)-coated MNPs (both γ-$Fe_2O_3$ and $Fe_3O_4$), PEG-coated $Fe_3O_4$ nanoparticles, and PEG-Au-coated $Fe_3O_4$ nanoparticles [103]. Neural MAPK/ERK and Caspase-3 levels were analyzed after intraneural injection, indicating inflammation and apoptosis. Both markers exhibited a significant increase in all animals injected with magnetic nanoparticles. However, there are also reports indicating the absence of significantly toxic effects of specific types of magnetic nanoparticles on the brain. For example, a study by J. S. Kim et al. involved the treatment of male ICR mice with silica-coated MNPs [104]. The mice were intraperitoneally administered three different concentrations of MNPs@SiO2, namely 100, 50, and 25 mg/kg, over 4 weeks. The study's findings established the capability of MNPs@$SiO_2$ to penetrate the blood-brain barrier (BBB) without compromising its functionality. Moreover, histological examinations and clinical biochemistry tests revealed no notable changes or macroscopic lesions in the organs, including the brain, in the MNPs@$SiO_2$-treated groups.

Intriguingly, magnetic nanoparticles may alleviate the toxicity of drugs in the brain. Fouad et al. tested the neuroprotective potential of sulforaphane (SF) loaded within $Fe_3O_4$ against cisplatin-induced neurotoxicity [105]. The study demonstrated that SF-MNPs significantly reduced acetylcholinesterase activity, alleviated oxidative stress, and ameliorated behavioral outcomes. These results were corroborated by histopathological features, confirming the safe toxicological profile of $Fe_3O_4$ nanoparticles.

The research findings on the neurotoxicity of magnetic iron oxide nanoparticles are often contradictory. This inconsistency can be attributed to a range of factors that influence the potential toxicity of the nanoparticles, including their physicochemical properties, surface chemistry, size, dosage, method of administration, and experimental model. Notably, several studies have indicated

 doi:10.20944/preprints202410.0530.v1



the potential neurotoxicity of MNPs, underscoring the necessity for further comprehensive investigations to elucidate and characterize this impact.

### *3.2. Heart and Circulatory System*

The specific molecular mechanisms of cardiotoxicity of magnetic iron oxide nanoparticles are not yet fully understood. However, it is widely accepted that the primary cause of heart toxicity is the generation of free radicals by these nanoparticles. *In vitro* experiments have revealed that nanoparticles significantly elevate oxidative stress damage, leading to overactivated autophagy and endoplasmic reticulum stress, ultimately resulting in cardiomyocyte apoptosis [106]. A proposed hypothesis suggests that the inclusion of antioxidants could effectively mitigate the cardiotoxic effects of the nanoparticles. N-acetylcysteine (NAC), known for its potent antioxidant properties, was integrated into mesoporous silica nanoparticles (M-MSN) to create M-MSN@NAC with a magnetic ($Fe_3O_4$) core [106–108]. The M-MSN@NAC treatment significantly reduced the oxidative stress of H/R cardiomyocytes induced by MNPs. This effect was attributed to the release of NAC, which effectively restricted the formation of peroxidation products. Significantly, the negatively charged nanoparticles did not substantially impact the actin skeleton of the heart cells, in contrast to their detrimental effect on the brain [109]. Nevertheless, adverse effects and cardiotoxicity associated with iron oxide nanoparticles have also been documented. For example, research has shown that the intravenous administration of polyacrylic acid-coated $\gamma$-$Fe_2O_3$ nanoparticles resulted in a decrease in mean arterial blood pressure (MAP) in healthy BALB/cJ mice [110]. In pigs, dimercaptosuccinic acid-coated MNPs (12 nm) administered intravenously at doses of 0.5 or 2.0 mg/kg induced a transient but significant reduction in MAP [111]. In a separate study, Manickam et al. tested the cardiotoxicity of $Fe_2O_3$-MNPs (< 50 nm) in mice [112]. A significant accumulation of MNPs was detected in the hearts of animals after 30 days of administration at doses of 25 and 50 mg/kg. Exposure to these particles resulted in oxidative myocardial damage. As a result, the researchers observed harmed mitochondria, decreased ATP levels, and overexpression of NOX4. Additionally, the authors suggested that mice treated with 50 mg/kg experienced both necrosis and apoptosis. Nemmar et al. examined the impact of 5 nm $Fe_3O_4$ with PEG stabilizing ligands on the heart and circulatory system [113]. Following the intravenous administration of nanoparticles at doses of 2 μg/kg and 10 μg/kg, a notable reduction in thrombotic occlusion time was observed in BALB/C mice's pial arterioles and venules. Furthermore, the presence of $Fe_3O_4$ nanoparticles led to a marked and dose-dependent increase in plasma levels of LDH, creatine phosphokinase-MB (CK-MB), and troponin-I, indicative of myocardial membrane damage. Elevated levels of ROS and DNA damage in the heart tissue were also noted at all studied doses of the nanoparticles.

Several reports have suggested that the immobilization of anticancer drugs on magnetic nanoparticles (MNPs) or the construction of carrier systems with a magnetic core may lead to a reduction in the cardiotoxicity of cytostatics. For example, Shetake et al. developed nano-formulations of magnetic nanoparticles co-encapsulated with doxorubicin (DOX) and indocyanine green (ICG) in a liposomal carrier (T-LMD), demonstrating minimal toxicity to heart tissue [114]. This is in contrast to DOX, which is known for its significant cardiotoxic effects [115,116]. In another study, a curcumin-loaded magnetic hydrogel nanocomposite was found to exhibit cardioprotective effects against doxorubicin-induced cardiac toxicity in rat cardiomyocytes [117]. Additionally, MNPs coated with DOX-conjugated heparin were found to be significantly less harmful to cardiac tissue in mice compared to free DOX at the same dosage [118]. Moreover, Xiong et al. designed and evaluated 2,3-dimercaptosuccinic acid-coated MNPs as potential agents for the treatment of cardiovascular diseases, concluding that these nanostructures showed promise as nanomaterials for protecting the heart from ischemic damage [119].

### *3.3. Liver, Spleen, and Lymph nodes*

The comprehensive investigation of magnetic nanoparticles' toxicity towards the liver and spleen is essential, as these organs serve as the primary capture and biodistribution sites for MNPs in both the short and long term [120]. Kupffer cells, a specialized population of liver macrophages,

 doi:10.20944/preprints202410.0530.v1



are responsible for the phagocytosis of pathogens, including MNPs, entering from the bloodstream. Additionally, the spleen plays a crucial role in removing pathogens and foreign particles, making it important to understand the impact of MNPs on this organ. Moreover, when administered intramuscularly or subcutaneously, regional lymph nodes may serve as the initial filter site for MNPs. High levels of alkaline phosphatase (ALP), alanine aminotransferase (ALT), and aspartate aminotransferase (AST) are typically indicative of liver damage. Additional markers for hepatic impairment involve hepatic plasma malondialdehyde (MDA), lactate dehydrogenase (LDH), tacrolimus (TAC), glutathione reductase (GSH), and gamma-glutamyl transferase (GGT) [121]. Examination of these enzyme profiles is typically performed in toxicity studies. Furthermore, histological analysis of the liver is considered a standard procedure. Askri et al. conducted a study investigating the impact of exposure to sub-acute MNPs (30 nm) at a 10 mg/kg dosage on Wistar rats [122]. The study revealed a notable decrease in alkaline phosphatase levels in rats exposed to MNPs, while no significant changes were observed in the levels of other hepatic enzymes (ALT and AST). In another study, the hepatotoxicity of dextran-coated iron oxide nanoparticles and dextran-coated MNPs conjugated with quercetin was studied in Wistar rats [123]. The study results revealed that there were no significant differences in the levels of AST, ALT, ALP, GGT, and LDH between the control group and the groups that received 50 and 100 mg/kg of quercetin-conjugated, dextran-coated MNPs in the liver. Administering dextran-coated magnetic nanoparticles at 100 mg/kg markedly reduced hepatic GSH level and CAT activity. Furthermore, there was a significant increase in hepatic MDA levels, while the hepatic TAC, GSH levels, MDA levels, and CAT activity exhibited no significant variances compared to the control group. These findings support the conclusion that quercetin effectively mitigated the toxic effects of MNPs and safeguarded the liver from oxidative damage. In a separate study, an investigation was conducted on the toxicity of 10 nm MNPs coated with the fourth generation (G4) of polyamidoamine (PAMAM) dendrimer toward BALB/c mice [124]. The histopathological results revealed edema and cytoplasmic depletion in the liver cells at a dosage of 10 mg/kg. Yaremenko et al. tested the toxicity of magnetic nanoparticles (50 nm) coated with glucuronic acid in BALB/c mice [125]. The histological analysis indicated that the injection of nanoparticles had no discernible effect on liver morphology on days 1, 7, 28, and 56. However, on day 14 post-injection, an increase in non-epithelial cells, particularly Kupfer cells and lymphocytes, was observed. Additionally, hemosiderin deposits were noted on days 1, 7, and 14 following the injection. Subsequently, the number of iron-positive cells decreased after 28 days, and on day 56, only small extracellular deposits of hemosiderin were evident, likely attributed to the demises of macrophages loaded with the nanoparticles. In the spleen, no morphological pathologies were observed on day 1 post nanoparticle injection. However, after 7 days, hyperplasia of the white pulp and an increase in lymphoid nodules were noted. After 56 days, an increase in red pulp cellularity and the number of megakaryocytes was observed. Similar to the liver tissue, hemosiderosis of the spleen was observed throughout the 8-week experiment post-Perls staining. Paulini et al. investigated the toxicity of DMSA-coated magnetic nanoparticles (11 nm) in rats, administered at doses of 0.5 or 5 mg Fe/kg, with long-term monitoring [126]. It was reported that no changes in serum ALT and AST were associated with DMSA-MNPs administration. Furthermore, all animals showed normal liver and spleen histology 10 months after DMSA-MNPs injection. However, recent studies have indicated that the administration of $Fe_3O_4$ nanoparticles, synthesized using *D. mucronate* leaves, at 100 or 300 mg per kg of a mouse's body, induced alterations in the liver and spleen tissues, with more pronounced effects observed at the higher dosage [127]. In these tissues, edematous, dilation of blood vessels and sinusoids were observed. Additionally, sinusoids have lost their original organization due to bio-$Fe_3O_4$ MNPs (300 mg/kg) accumulation compared with control and 100 mg/kg bio-$Fe_3O_4$ MNPs injection.

Magnetic nanoparticles exhibit substantial accumulation in lymph nodes, thus holding promise for early cancer detection in the lymphatic tissues. MNPs with a hydrodynamic diameter ranging from 20 to 30 nm demonstrate an extended circulation period, rendering them valuable for applications in lymphography, inflammation, and blood pool imaging [128]. Extensive research is currently underway to explore the potential application of MNPs as nanotheranostics in the

 doi:10.20944/preprints202410.0530.v1



treatment of cancer lymph node metastasis [129]. Regrettably, there is a paucity of comprehensive studies on the potential toxicity of MNPs to lymph nodes, and the available studies on this matter are notably limited. A particular report evaluated carboxylic mannan-coated MNPs (CM-MNPs) with a 34 nm size, designed to target immune cells for lymph node-specific MRI *in vivo* [130]. The mice administered with CM-MNPs did not show any abnormalities. The LD50 of CM-MNPs was found to be more than 80 mg Fe/kg in mice, indicating the safety of the studied nanostructures. Sekino et al. developed a handheld magnetic probe with a permanent magnet and Hall sensor to identify sentinel lymph nodes (SLN) in breast cancer patients [131]. Histopathology confirmed the accumulation of the MNPs (Resovist, 60 nm, carboxydextran shell) in the cortex of the extracted node. However, the authors did not present possible changes or potential toxicity effects caused by nanostructures in this tissue. In another study, polyacrylic acid-modified iron oxide nanoparticles (PAA@MNPs) were studied as potential agents for differentiating between hyperplastic and metastatic breast cancer lymph nodes [132]. The authors reported no negative effects on body weight, hematology, coagulation parameters, serum biochemistry, and gross anatomy of all Sprague-Dawley rats after receiving single or multiple doses of PAA@MNPs via intravenous administration. Additionally, histopathological examination revealed no abnormal findings.

### *3.4. Respiratory System*

Magnetic iron oxide nanoparticles are the subject of extensive research due to their potential applications in lung disease diagnostics and therapies. Therefore, it is crucial to thoroughly examine their potential toxicity to lung tissue. Kubovcikova et al. examined the potential of N-acetylcysteine (NAC) immobilized on poly-L-lysine-functionalized iron oxide magnetic nanoparticles (NAC-PLL-MNPs, 10-11 nm) for enabling magnetic resonance imaging of drug distribution in the lungs [133]. NAC is a pharmaceutical approved by the FDA and recognized by the WHO as an essential medication. It is extensively utilized for treating acetaminophen overdose and, more recently, as a mucolytic agent in respiratory diseases [134]. PLL-MNPs and NAC-adsorbed PLL-MNPs displayed excellent MRI contrast properties, allowing for the differentiation between magnetic nanoparticles with and without immobilized NAC [133]. Cytotoxicity experiments on the obtained nanostructures were carried out using an LDH assay kit on the HEK cell line at concentrations of 0.1, 10, and 50 μg/ml. No cell toxicity was observed after 24 or 48 hours of incubation at any of the three concentrations. However, it is notable that the researchers did not examine toxicity specifically in lung tissue. In a distinct study, the biological impact of green-synthesized MNPs on two different lung tumorigenic monolayers (A549 cells - lung carcinoma with an epithelial-like morphology and NCI-H460 cell line - large lung cancer cells) and a 3D normal bronchial model was investigated [135]. The MTT assay showed that 24 hours after treatment, none of the test samples significantly reduced the viability of the 3D microtissues, with viability rates above 80%. The 3D models treated with MNPs exhibited some superficial layer damage, but no damage to the microporous membrane or loose epithelial junctions was observed. Additionally, no histopathological changes were noted. In conclusion, MNPs synthesized using green methods were found to be non-toxic to bronchial epithelia when applied at a concentration of 500 μg/ml. As for the antitumoral activity of the obtained MNPs on two human lung carcinoma cell lines, the Alamar blue test showed that the viability of the A549 cell population was more affected compared to the viability of NCI-H460 cells. The efficacy of tumor-targeted magnetic nanoparticles for magnetic hyperthermia treatment of non-small cell lung cancer (NSCLC) in mice via inhalation was evaluated by Sadhuka et al. [136]. The study findings demonstrated the high accumulation of EGFR-targeted MNPs (EGFR- Epidermal Growth Factor Receptor) in the pulmonary tissues. Furthermore, the administered mice exhibited no distress symptoms over the 30-day study period, suggesting the absence of acute systemic toxicity or harm to healthy lung tissue. In a separate report, the study presented results regarding the efficacy of MNPs in the treatment of bacterial pneumonia [137]. Vancomycin (VAN) was affixed to the core of magnetic nanoparticles, followed by spray-drying onto lactose/dextran. Subsequent *in vivo* safety and pharmacokinetic assessments validated the pulmonary tissue localization of VAN-coated MNPs and evidenced a reduction in adverse effects in comparison to free VAN.

 doi:10.20944/preprints202410.0530.v1



Numerous types of magnetic nanoparticles tend to accumulate in the lungs, even when the lung tissue is not the primary target for MNPs in potential therapies for the respiratory system. For instance, several reports have documented the biodistribution of dimercaptosuccinic acid (DMSA)-coated MNPs. Typically, these nanostructures do not adversely affect cell viability *in vitro* [138]. One significant concern pertains to the potential impact of such nanoparticles on organs in the context of biological procedures. For instance, investigations conducted on mice demonstrated that, following intravenous injection, DMSA-MNPs were primarily concentrated in the lungs. These nanoparticles were observed in the blood vessels within the lungs, subsequently in the capillaries, and ultimately within parenchyma cells. Additionally, some nanoparticles were detected in the cytoplasm of macrophages within the bronchiolar lumen. The presence of DMSA-MNPs in the lungs contributed to heightened levels of interleukin-1 and interleukin-6, triggering an inflammatory process [139]. Mild inflammation of the lung parenchyma was observed up to 15 days after DMSA-MNP administration, with an apparent increase in the number of inflammatory cells distributed throughout the parenchyma. In a separate study, an investigation was conducted to examine the long-term impacts of DMSA-MNPs on the organs of rats [126]. The study findings indicated a mild interalveolar septal thickening in the lungs; however, the animals did not display any clinical respiratory symptoms. Askri et al. investigated the effects of sub-acute exposure to 30 nm MNPs on Wistar rats [122]. The animals were administered intranasally at a dosage of 10 mg/kg body weight. The findings indicated that MNPs had no observable effect on the structure of the lungs.

### *3.5. Urinary system*

Investigating renal clearance of magnetic iron oxide nanoparticles is of significant interest in minimizing the systemic toxicity of MNPs [140]. The nanoparticles need to overcome the glomerular filtration barrier in order to be effectively eliminated by the kidneys in their pristine state. This process is particularly efficient for MNPs with a hydrodynamic diameter below 6 nm [141,142]. The research conducted by Wei et al. involved the fabrication of 3 nm $Fe_3O_4$ nanoparticles, which were subsequently coated with dopamine sulfonic acid, resulting in the formation of 4.7 nm nanostructures [143]. The obtained MNPs demonstrated good $T_1$ contrast agent properties and facilitated rapid metabolism through the mice's kidneys. Liu et al. synthesized amphoteric conjugated hollow $Fe_3O_4$ nanoparticles measuring 7 nm in size [144]. These nanoparticles held potential as $T_1$ contrast agents and demonstrated rapid and complete clearance by the kidneys. Both reports' authors confirmed the biosafety of the nanostructures. In another study, a renal-clearable ultra-small ferrite nanoprobe (UMFNPs@ZDS) was proposed for highly sensitive early diagnosis of kidney damage using structural and functional MRI *in vivo* [145]. The nanostructures consisted of a ferrite core coated with a zwitterionic layer and had a high $T_1$ relaxivity and a small hydrodynamic size (6.43 nm). In cytotoxicity studies utilizing the MTT assay against the HK-2 cell line, which is an immortalized proximal tubule epithelial cell line derived from a normal adult human kidney, it was observed that cell viability remained above 80% even when exposed to a high concentration of UMFNPs@ZDS (200 μg/mL). Moreover, subsequent histopathological evaluation following the administration of the nanoprobe to rats revealed the absence of noteworthy lesions in vital organs, including the kidneys. However, there is an ongoing concern regarding the kidney toxicity of magnetic nanoparticles with larger sizes and different surface chemistry. Several articles have documented the potential toxicity of MNPs to various organs, including the urinary system. In a study by Alalaq et al., $Fe_2O_3$ nanoparticles of varying sizes (45 to 46 nm) were orally administered to mice every 48 hours for 60 days [146]. The histological analysis of different segments of the mice' kidneys revealed no evidence of kidney damage at lower concentrations (6 and 8 μg/L in drinking water) of nanoparticles. However, 100- and 120 μg/L concentrations resulted in noticeable structural changes and congestion between the tubules. Additionally, damage to cells in the proximal tubules and the epithelial lining of the distal convoluted tubules was observed. Another study investigated the nephrotoxicity of dextran-coated MNPs and quercetin-conjugated MNPs (QMNPs) in Wistar rats [123]. Quercetin is considered a versatile molecule due to its wide range of clinical effects, including inhibiting carcinogenesis and reducing cardiovascular diseases [147]. The study results by Kazemipour et al.

 doi:10.20944/preprints202410.0530.v1



showed that renal catalase (CAT) activity significantly increased in the group that received 100 mg/kg of MNPs-quercetin, while it significantly decreased in the group that received 100 mg/kg of dextran-coated MNPs compared to the control group [123]. However, the levels of renal tacrolimus (TAC), glutathione reductase (GSH), and plasma malondialdehyde (MDA) were not significantly different among the groups. The 100 mg/kg dextran-coated MNPs did not cause any oxidative injury to the kidneys. In a separate study, researchers assessed the effects of 40-nm MNPs on renal function [125]. The histopathology analysis indicated no morphological changes in the organs following 28 days of administering nanoparticles to BALB/c mice. However, on day 56, a dystrophic change was observed in the epithelium of several tubules. Furthermore, after Perls staining on day one post nanoparticle injection, diffuse blue staining was observed in the epithelium of some kidney tubules, primarily located in the luminal area of the cells. Nonetheless, these changes had disappeared by days 28 and 56. It was postulated that excess iron in the kidneys may have resulted from the non-specific accumulation of the smallest nanoparticles and their subsequent degradation. In a study by Attia and Thalij, the impact of MNPs and chitosan-coated MNPs on kidney function parameters (creatinine and urea) in male albino rats induced with anemia using phenyl-hydrazine was assessed [148]. The findings revealed elevated levels of creatinine and urea in the rats induced with anemia, indicative of renal impairment. However, the administration of MNPs and chitosan-coated MNPs to the anemia-induced rats resulted in sustained normal levels of kidney parameters

### *3.6. Reproductive system*

Magnetic iron oxide nanoparticles demonstrate promise for diagnosing and treating reproductive system diseases. For instance, MNPs attached to *Arachis hypogea* lectin/*Pisum sativum* lectin (PNA/PSA lectin) have been utilized to detect defective spermatozoa during the selection process [149]. In another study, MNPs conjugated with Annexin V and lectin were utilized to isolate apoptotic and acrosome-activated sperms from their healthy counterparts in boar and camel [150,151]. It was also reported that MNPs have proven valuable tools in monitoring human mesenchymal stem cells transplanted into the penile cavernosum of rats with erectile dysfunction [152]. In conclusion, the precise engineering of magnetic nanoparticles enables the development of safe nanoscale vesicles to treat reproductive system disorders. Nonetheless, there are documented instances regarding the adverse effects of iron oxide nanoparticles on the reproductive system. In a study conducted by Sundarraj et al., the potential toxicity followed by repeated administration $Fe_2O_3$ nanoparticles on the testes of mice was investigated [153]. The study observed the accumulation of these nanostructures in the testes following exposure. Administration of 25 and 50 mg/kg of nanoparticles resulted in elevated levels of reactive oxygen species, lipid peroxidation, protein carbonyl content, glutathione peroxidase activity, and nitric oxide, while concurrently decreasing the levels of antioxidants such as superoxide dismutase, catalase, glutathione, and vitamin C. The study also noted apoptosis, along with higher concentrations of MNP exposure, leading to an increase in serum testosterone levels. In a separate study, pregnant mice were intraperitoneally injected with varying doses of MNPs coated with dimercaptosuccinic acid (DMSA) [154]. The study results indicated that doses exceeding 50 mg/kg of DMSA-coated magnetic nanoparticles could interfere with embryo development. Al-Shammari and Al-Saaidi studied the impact of magnetic nanoparticles on male rat reproduction, considering both dosage and duration of exposure [155]. The animals were administered with MNPs solution orally at doses of 1 (TL group), 5 (TM group), and 10 (TH group) mg/kg/day for 28 days. The results showed a significant decrease in the relative weights of the testis, epididymis, prostate, and seminal vesicle in the TH and TM groups compared to the control group. In contrast, no significant change was observed in the TL group. Histopathological studies revealed degenerative changes and a reduced population of germinal epithelium in the TM and TH groups. Additionally, vacuolation, necrosis, hyaline degeneration of spermatogonia, decreased number of spermatocytes, and hyperplasia of Sertoli cells were observed. Furthermore, there was a significant increase in testicular luteinizing hormone receptor (LHR) gene expression levels in the TL group, while the TM and TH groups exhibited a significant decline relative to the control group. The effect on the endocrine system was confirmed by evaluating hormone concentrations in serum. The

 doi:10.20944/preprints202410.0530.v1



concentrations of gonadotropin-releasing hormone (GnRH), follicle-stimulating hormone (FSH), luteinizing hormone (LH), and testosterone in male rats from the TH group were the lowest, followed by male rats from the TM group, compared to male rats in the control group.

*3.7. Skin*

One of the primary pathways for the entry of nanoparticles into the body involves absorption through the skin. Consequently, the presence of iron oxide nanoparticles can influence the functions of this organ. Penetration of MNPs into healthy skin entails the generation of free radical, oxidative stress and collagen depletion [156,157]. Following dermal exposure to nanoparticles, subsequent physiological responses may encompass keratinization, dermal atrophy, and the manifestation of skin wrinkling. However, comprehensive investigation into the cutaneous toxicity of magnetic nanoparticles remains scarce. A study conducted by Amin et al. evaluated the cytotoxic potential of 54 nm magnetic nanoparticles on both normal and malignant human skin cells by employing the MTT assay [158]. The cell lines included human dermal fibroblasts, human squamous cell carcinoma cells (A431 cells), and human epidermal keratinocytes (HaCaT cells). The research results indicated that, within the tested concentration range (10 μg/mL to 500 μg/mL), $Fe_3O_4$ nanoparticles demonstrated negligible impact on all investigated cells.

Iron oxide nanoparticles can have great potential in the treatment of skin diseases. For instance, Duval et al. evaluated the protein and gene expression of B16 melanoma mouse cells following medium magnetic hyperthermia [159]. Melanoma cells were collected and combined with MNPs and then exposed to an alternating magnetic field (AMF). The findings demonstrated a marked upregulation of the HSP70 gene, associated with enhanced heat tolerance and immunogenicity, as well as alterations in specific receptor gene pathways linked to adsorbent chemistry and toll-like receptors. Furthermore, in a separate study, a hydrogel incorporating dextran-coated iron oxide nanoparticles (DEX-MNPs) was proposed and evaluated as a potential vehicle for topical photothermal therapy (PTT) in the treatment of skin cancer [160]. Preliminary efficacy studies in the B16F10 s.c. mice models have shown that the use of DEX-MNPs gel in topical PTT can significantly reduce tumor volumes. Simultaneous treatment involving a single PTT session with 100 μgFe/mL DEX-MNPs gel and applying 0.5 W laser power for 10 minutes resulted in an 85% significant inhibition of tumor growth.

The summary of magnetic nanoparticles' toxicity towards different models and with varied properties is presented in Table 1.

**Table 1.** The summary of the toxicity of diverse MNPs toward different models.

| Size (TEM/$D_H$) | Coating | Model | Dose | Significant methods for toxicity assessing | Toxicity | Ref |
|---|---|---|---|---|---|---|
| 212 nm/- | DOX[1]-4, 4'-Azobis (4 - cyanovaleric acid) | ICR mice | 200 μl of solution of free DOX and DOX-loaded MNPs at a dose normalized to be 3 mg/kg DOX equiv. | Histology | MNPs-Azo-DOX did not produce histopathological signs of cardiotoxicity like that observed for free DOX. | [167] |
| -/50 nm | Rhodamine B isothiocyanate (RITC) within a silica shell | ICR mice | 100, 50, 25 mg/kg | Blood biochemistry, hematology and histology<br>Neurotoxicity assays | No significant changes were observed in the histological, hematological, and biochemistry tests.<br>MNPs could penetrate the BBB without altering its function. | [103] |
| 12 nm/-<br>26 nm/- | Bare<br>Silica-APTES[2] | HeLa and A549 cells | 0.5, 1, 2.5, 5 nM | WST-8 assay<br>DCF fluorescence as a reporter of ROS generation | Bare MNPs showed a substantial viability reduction at high concentrations (2.5, 5 nM) in both cell lines, whereas coated MNPs showed no sign of toxicity. | [17] |

 doi:10.20944/preprints202410.0530.v1



| | | | | | | |
|---|---|---|---|---|---|---|
| | | | | | A significant ROS generation was observed in cells treated with bare MNPs. Coated MNPs induced low levels of ROS. | |
| -/10 nm<br>-/100 nm<br>-/150 nm | Bare<br>APTMS[3]<br>TEOS[4]/APTMS | HDFs and HT-1080 cells | 200–1000 µg/ml | Cell Counting Kit-8 assay<br><br>Comet assay | In HDFs treated with increasing concentrations of each MNPs in a dose-dependent manner, a slight toxicity was observed.<br>MNPs modified with APTMS resulted in significant dose-dependent genotoxicity against normal cells. Bare and TEOS/APTMS-coated MNPs resulted in neither extensive nor dose-dependent damage to the DNA stability in both cells. | [20] |
| -/60 nm | DMSA[5] | OLN-93 cells | 0.25, 1, 4 mM | LDH assay<br><br>Staining with PI, H33342, and rhodamine 123 dyes | No significant increase in the extracellular activity of the enzyme LDH was observed.<br>Cultures incubated with 0.25 or 1 mM MNPs hardly contained any PI-positive cells despite the presence of many cells which was demonstrated by H33342 staining. Exposure to 0.25 mM MNPs did not increase ROS production, while many rhodamine 123-positive cells were present in cultures exposed to 1 or 4 mM MNPs. | [168] |
| 6 nm/-<br>8 nm/- | Bare<br>Chitosan | HeLa, A549 and HeK293 cells | 0.5, 2, 4 µg/µl | MTT assay and AO/EB staining | The toxic effect of chitosan-MNPs on A549 and HeLa cells was moderate compared to bare MNPs treatment, and this toxicity was found to be time—and dose-dependent. In the case of Hek293 cells, bare MNPs led to toxic effects, whereas chitosan-coated MNPs did not cause any significant toxicity. Chitosan-MNPs caused less apoptosis in healthy and cancer cell lines than bare MNPs. | [18] |
| 10, 20, 30, 40 nm/14, 25, 34, 43 nm | Oleic acid | Kunming mice | 20 mg/kg | Blood biochemistry | The critical hepatic indicators were not significantly altered independent of the sizes of MNPs treated compared with the control. The kidney function indicators exhibited levels similar to those of the control group. | [169] |
| 4.5 nm/2-8 nm | PAA[6]-co-3-DEAPA[7] | HUVEC cells<br>Mice | Not available<br><br>0.2 ml of 0.138 mM solution | MTT assay<br><br>Histology | No toxicity was observed.<br><br>No abnormal changes were observed. | [170] |
| 10 nm/ 369 nm (N1)<br>10 nm/ 238 nm (N2) | Oleic acid-chitosan (N1)<br><br>Oleic acid-chitosan and glutaraldehyde as cross-linker (N2) | ECs cultures from Wistar rats<br><br>Mice | 1, 10, 100 µg/ml<br><br>30 mg/kg | MTT assay<br><br>Measurement of NO production | ECs treated with N1 nanoparticles for 6–24 h compared to control cells showed maximal cell viability. In contrast, a significant reduction in cell viability was evidenced in the treatment with the highest dose (100 µg/ml) after 36 h. The treatment with N2 MNPs did not affect cell viability in the whole range of doses and times explored.<br>Endothelial NO production was not affected by the exposure to N1 or N2. | [171] |
| 9.9 nm/ 406 nm | Curcumin | HUVEC cells | 200 µl of medium at concentrations 1-1000 µg/ml | A calcein AM red-orange viability assay | Curcumin-coated MNPs showed less cell death relative to uncoated MNPs at variable concentrations. | [172] |
| 34 nm/ 325 nm<br>270 nm/ 1100 nm | PEG[8] 2000<br><br>Ethylene glycol | D407, A548, MV35 and | 0.05–0.2 mg/ml | MTT assay | No significant toxicity was observed. | [173] |

 doi:10.20944/preprints202410.0530.v1



| | | | | | | |
|---|---|---|---|---|---|---|
| | | B12F10 cells | | | | |
| 10-50 nm (AFM) / 50 nm | Bare | Mouse embryonic fibroblasts NIH3T3 | 32.5 ng/ml | XTT assay | No significant toxicity was observed. | [174] |
| 10-20 nm/40-160 nm | Dextran | L929 fibroblast Albino rats (Wistar), Albino guinea pigs (Hartley), and Albino mice (Swiss) | 100- 800µg/ml<br><br>300-2000 mg/kg | MTT assay<br><br>Blood biochemistry and hematology<br><br>Lymphocyte proliferation assay<br><br>Detection of 8-OHdG by ELISA | No proliferation inhibition in the whole range of MNPs concentrations was observed.<br>The biochemical and hematological assessments following oral administration of MNPs were not significantly different from those in the control group.<br><br>Seven days after exposure, a slight increase in cell number was observed in both T and B lymphocytes compared to the control. After 14 days and 21 days, the proliferation of T and B cells was reduced compared to day 0.<br>The levels of 8-OHdG in mitochondrial DNA of MNPs exposed groups were comparable with that of control values. MNPs did not significantly affect the chromosome aberration frequencies in bone marrow cells or cell mitotic indices. | [41] |
| 8,17,24 nm/32.2, 51.8, 84.4 nm | Human-like collagen (HLC) protein | BHK-21 cells | 100 µl of 12.5-100 µg/ml | WST-8 assay using Cell Counting Kit-8 (CCK-8) | No toxicity was observed for all concentration ranges and sizes, regardless of their incubation time. | [175] |
| -/320 nm | Chitosan | ECs from Wistar rats<br>Human blood<br><br>F1 mice | 1-100 µg/ml<br><br>1, 10 and 100 µg/ml<br><br>30 mg/kg | MTT assay<br>NO production<br>The erythrocyte sedimentation rate and hematology<br>Histology | No viability inhibition of cells was observed.<br>The presence of the MNPs did not affect basal NO production.<br>No significant differences in ESR in comparison to controls were observed.<br>The hemolytic effect was not observed with any of the tested doses assayed.<br><br>Histological examinations of the liver, stomach, intestine, lungs, and brain showed no changes at the end of the sub-acute exposure to MNPs in any of the mice after 28 days. The kidneys exhibited granular interstitial tissue, which was compatible with periarteriolar interstitial nephritis compared to the control. In the spleen, an increase in the presence of megakaryocytes was observed. | [176] |
| -/80 nm<br>-/40 nm<br>-/40 nm | BSA[9]<br>BSA<br>BSA-PEG | Human fibroblast cells<br>Human glioblastoma U251 cells | $10^{-3}$ –$10^{-7}$ M | MTT assay<br><br>LDH assay<br><br>Oxidative activity evaluated by a dichloro-dihydrofluorescein | After 48 hours, the highest concentration of BSA-IONP-80 and BSA-IONP-40 showed some cytotoxic effect, which was more robust in the case of BSA-MNP-40. BSA-MNPs-PEG toxicity was almost negligible in comparison to other types of MNPs.<br>No significant change in the confluency area of U251 cells was observed.<br>The measurements of LDH activity after 24 hours of incubation with MNPs have not shown any differences in cell membrane integrity for all samples in all concentrations tested. | [19] |

 doi:10.20944/preprints202410.0530.v1



| | | | | | | |
|---|---|---|---|---|---|---|
| | | | | diacetate fluorescent dye. Comet assay | For 24 hours, all types of MNPs provided less ROS production than positive control. After 48 hours of HF-cells incubation, a noticeable increase in fluorescence level was observed. Signal intensity was almost equal to fluorescence intensity related to cells treated with a control solution of $H_2O_2$. As for U251 cells, a significantly lower fluorescence level was observed compared with the control solution of $H_2O_2$. 24 hours after incubation with different types of synthesized MNPs, there was no difference in DNA damage level between the control and experimental nanoparticles groups. An increase in DNA fragments was detected after 48 hours of HF-cells incubation with BSA-MNPs-40. In the case of the U251 cell line, no significant difference between DNA fragmentation in control and treated cells for all types and concentrations of MNPs used was observed. | |
| 10 nm /16.5 nm<br>30 nm/ 38.5 nm<br>10 nm/ 17.2 nm | PEG<br>PEG<br>PEI[10] | RAW264.7 macrophage, SKOV-3 cancer cells<br>BALB/c mice | 3.125 – 100 µg/ml<br>1.5 – 5 mg/kg | MTS assay<br>Hematology and blood biochemistry<br>Histology | SEI-10 induced dose-dependent cytotoxicity against both RAW264.7 macrophages and SKOV-3 cancer cells at the test concentrations, and SKOV-3 cells were relatively more susceptible to SEI-10 toxicity than RAW264.7 macrophages. No appreciable cytotoxic effects were observed for SMG-10 and SMG-30 at 25µg/mL; slight cytotoxicity was shown above 50µg/ml.<br>The hematology and blood chemistry results on day seven post-injection showed that AST, total bilirubin, BUN, and creatinine were within the normal range, except that the level of ALT enzyme in mice treated with SMG-10 slightly increased compared to the PBS control. On day 14 post-injection, the increased ALT level in SMG-10-treated mice returned to normal.<br>In mice treated with SMG-10 and SMG-30, slight mononuclear cell infiltration in the portal area of the liver was identified. Splenic plasmacytosis was noted in mice treated with SMG-30. | [177] |
| -/60 nm | L-glutathione | *Caenorhabditis elegans* - non-parasitic nematodes | 10-200 mg/l | Mortality<br>Growth<br>Locomotion<br>Fertility | The presence of nanomaterial increased mortality without a specific relationship between the concentration and the number of dead nematodes. A slight decrease in the length of the worms was observed for the control. A decrease in locomotion was not significant. A decrease in the number of eggs placed was observed for each nematode by increasing the nanomaterial concentration in the medium. | [178] |

 doi:10.20944/preprints202410.0530.v1



| | | | | | | |
|---|---|---|---|---|---|---|
| 24.33-34.24 nm/- | Curcumin-PEG | MCF7 cells<br>Human red blood cells | 1-100 µg/ml<br>10 mg/ml | MTT assay<br>Hemolysis assay | MNPs did not show any toxicity.<br>Non hemolytic response was observed. | [179] |
| 12 nm/ 40 nm (PA)<br>12 nm/ 72 nm (HA) | PA-PEG phosphonic acid<br>HA-PEG hydroxamic | Primary human peripheral leucocytes | 0.12–75 µg/cm | Measurement of $^{3}$H-thymidine incorporation into DNA of cells | No significant cytotoxic effect of PA-PEG@MNPs and HA-PEG@MNPs) was found after 24 and 72 hours of incubation. | [180] |
| 3 nm/ 21 nm 14-20 nm/56 nm | PEG | Mouse microglia cell line N13<br>Zebrafish embryos | 0.1-100 µg/ml<br>0.01-100 µg/ml | MTT assay<br>Evaluation of the hatching and survival rates of zebrafish embryos | No significant cytotoxicity after 24 h of exposure to any MNPs was observed.<br>Higher concentrations of MNPs (10 µg/ml and 100 µg/ml) showed an increased hatching rate compared to control non-exposed embryos. No mortality or malformations were observed in the embryos exposed to different doses of particles at 48 hours. | [181] |
| 18 nm/ 230 nm | PEG-Arginine | HFF2 and HEK293 cells<br>Human red blood cells | 0.06-0.40 mg/ml<br>10 mg/ml | MTT assay<br>Hemolysis assay | No significant cytotoxicity after exposure to any MNPs was observed.<br>MNPs did not affect HRBCs of the blood. | [182] |
| 9 nm/ 11.68 nm Nano-clusters of 100-150 nm/- | Bare MNPs<br>pPEG-AC[11]-poly(amidoamine- paraben-PEG | Swiss albino mice | 5, 10, and 25 mg/kg | Blood biochemistry .<br>Histology | The highest dose of bare MNPs induced significant malfunctions in systemic biomarkers. In contrast, lower doses (5 and 10 mg/kg) of uncoated and all coated MNPs did not alter these biomarkers.<br>All tissue sections, including liver, kidney, spleen, and heart, excluding lungs, treated with the highest dose (25 mg/kg) of bare MNPs demonstrated significant iron deposition. Lower doses (5 and 10 mg/kg) of uncoated MNPs and all coated NPs showed no iron accumulation. | [15] |
| -/120 nm | L-carnosine | BALB/c mice | Equivalent carnosine dose of 200 mg/kg/day | Blood biochemistry<br>Histology | A significant increase in the liver enzymes (ALT and AST) was observed.<br>Iron accumulations were detected. No structural or histopathological changes were observed in the liver tissues, indicating no tissue damage. | [183] |
| -/147 nm -/116.5 nm -/139 nm | PEI<br>PAH[12]<br>PDADMAC[13] | Human lung carcinoma cell line (A549). | 100 µg/ml | MTT assay<br>Resazurin reduction assay | The MTT test showed a slight decrease in the activity of cytosolic hydrogenases in all variants, most pronounced in the variant with MNPs-PEI.<br>A test with resazurin reduction showed that incubation with MNPs-PEI slightly stimulated mitochondrial enzymes. | [184] |
| 9.2 nm/ | PAA-CF[14] | Splenic cells from rat<br>Albino mice | 7.8 -1000 µg/ml<br>Single dose of 100 µg/ml PAA@CF-MNPs | Trypan blue dye exclusion method and MTT assay<br>Blood biochemistry | Non-significant cell growth stimulatory effects were observed at 1000, 62.5, 15.6, and 7.8 µg/ml and non-significant cell growth inhibitory effects at 500, 250, 125, and 31.25 µg/ml.<br>The levels of ALT and AST showed a non-significant increase over the usual control group. The renal function parameters (serum urea and creatinine) were normal. | [185] |

 doi:10.20944/preprints202410.0530.v1



| | | | | | | |
|---|---|---|---|---|---|---|
| Not available | Ag/$Fe_3O_4$-CS[15]-PVA[16]/Ag | HEK293 and LO2 cells<br>Mice | 1.25-40 µg/ml<br>Not available | Cell counting kit-8 assay<br>Hemolysis<br>Histology | No apparent toxic effects on cells were observed.<br>Slight hemolysis was observed.<br>No abnormal changes were observed. | [186] |
| 46-57 nm/- | Carboxymethyl chitosan | MCF7 human breast cancer cells and 3T3 fibroblasts | 6.25-100 µg/ml | MTT assay | MNPs displayed toxic effects against MCF-7 cells. No toxicity towards 3T3 fibroblasts was observed. | [187] |
| 2-5 nm/- | ε-Poly (L-lysine) carbon dots | Mouse MC3T3-E1 cells<br>Human red blood cells | 0.1, 0.5, 1 mg/ml | Cell counting kit-8 assay<br>Homolysis | No toxicity was observed.<br>Low concentrations of MNPs (0.1 mg/ml) possessed acceptable hemocompatibility. | [188] |
| 12-15 nm/98 nm | Curcumin/ Alginate | Sarcoma 180 cancer cells<br>Mice | 0.01-1000 µg/mL<br>80-120 mg/kg | MTT assay<br>Blood biochemistry<br>Histology | The cytotoxicity was observed only at high doses.<br>Biochemical assay data indicated that AST and ALT values were higher in the treated mice than in the control mice, with a significant difference in AST values. In contrast, the levels of BUN and creatinine did not change significantly.<br>The histological structures of livers changed compared to those in the control group, with the appearance of vacuolated hepatocytes. | [189] |

[1]DOX – doxorubicin; [2]APTES – (3-aminopropyl)triethoxysilane; [3]APTMS – (3-aminopropyl)trimethoxysilane; [4]TEOS – tetraethoxysilane; [5]DMSA – dimercaptosuccinic acid; [6]PAA -poly(acrylic acid); [7]DEAP – 3-(diethylamino)-propyl amine; [8]PEG – poly(ethylene amine); [9]BSA – bovine serum albumin; [10]PEI – poly(ethylene imine); [11]AC – aminocellulose; [12]PAH – poly(allylamine hydrochloride); [13]PDADMAC – poly(diaallyldimethylammonium chloride); [14]CF – cobalt ferrite; [15]CS – chitosan; [16]PVA polyvinyl alcohol;.

## 6. Conclusions and Future Perspectives

The use of magnetic iron oxide nanoparticles in drug delivery and theranostic applications has garnered significant attention in recent years. Thus, it is imperative to diligently evaluate the potential toxicity of the nanoparticles intended for medical purposes. Nanotoxicity is influenced by various factors, including the dimensions and morphology of the nanoparticles, their surface chemistry, and charge, as well as their interactions with components of blood serum, biodistribution, and clearance within the biological system. Technical parameters such as dosage, exposure duration, frequency of administration, and the precursors utilized in nanoparticle preparation also substantially influence toxicity. Moreover, nanoparticles with similar properties may exhibit varying toxicity in disparate experimental models. An in-depth understanding of molecular-level interactions is pivotal in elucidating nanoparticle toxicity towards specific tissues and organs. The primary mechanisms and factors contributing to nanotoxicity encompass oxidative stress, interactions with genetic material, dysregulation of gene expression, cell membrane disruption, alterations in the cell cycle, inflammatory responses, disturbances in iron homeostasis, and cellular motility. When developing magnetic nanoparticles for medical purposes, researchers commonly adhere to fundamental principles aimed at minimizing nanoparticle toxicity. For instance, the application of surface functionalization with biocompatible polymers such as PEG is recognized for its ability to significantly diminish nanoparticle toxicity. This is predominantly rationalized by the limitation of free iron ions release and the altered interactions of MNPs with negatively charged cellular membranes [161]. In a recent study, magnetic $Fe_3O_4$ nanoparticles functionalized with (3-aminopropyl)triethoxysilane (APTES) or N-carboxymethyl chitosan (CMC) were suggested as potential nanocarriers for methotrexate (MTX) to specifically target ovarian cancer cell lines [162].

 doi:10.20944/preprints202410.0530.v1



These polymer modifications were observed to effectively mitigate the toxicity of the nanoparticles, as evidenced by the lack of cell proliferation inhibition in the MTT assay. An alternative method to modulate nanoparticle interactions with cell membranes involves the manipulation of nanoparticle morphology. Additionally, morphology may be correlated with the dissolution of the material [163]. The dissolving rate of particles is influenced by their various morphologies, surface areas, crystal planes, and particle curvature. Particles with smaller curvature radii are less energetically favorable and thus prone to undergo more dissolution. Therefore, it can be inferred that morphologies such as nanorods may exhibit lower toxicity compared to nanospheres, as their dissolution rate is expected to be slower.

One strategy for mitigating the toxicity of MNPs resulting from oxidative stress involves concurrently administering various antioxidants during nanoparticle therapy. Ucar et al. demonstrated that using ulexite (UX) at a concentration of 18.75 mg/l as a natural therapeutic agent effectively reduced oxidative stress in brain tissue [164]. On the other hand, MNPs conjugated with quercetin (QC) promoted neurogenesis without any toxicity [165]. The research findings elucidate that the QC inhibited protein aggregation and acted against iron overload via iron-chelating activity, iron homeostasis genes regulation, radical scavenging, and attenuation of the Fenton/Haber–Weiss reaction. Another study revealed that lipoic acid exhibited potent antioxidant properties by effectively scavenging hydroxyl radicals generated in the Fenton reaction involving Fe(II) [166].

Despite the aforementioned general principles, it is essential to note that nanotoxicity is influenced by a multitude of factors. Therefore, each type of designed nanoparticles should undergo thorough and separate testing. Typically, initial toxicity tests are conducted *in vitro*. Establishing an *in vitro* model for toxicity study is imperative for determining appropriate dosage and concentration levels for further evaluation in an *in vivo* system. Consequently, *in vivo* studies are essential for discerning the actual and final nanotoxicity impact on the body.

Magnetic nanoparticles constitute a burgeoning study area with extensive potential in numerous medical applications. The imperative for precise targeting, coupled with the escalating challenge of drug resistance in treating specific cancerous tissues, underscores the necessity for targeted approaches employing MNPs. Significantly, MNPs can selectively impact healthy and cancerous cells, precipitating the termination of solely the cancerous cells, which is a highly desirable attribute in cancer treatment. Nanoparticles can be functionalized with various specific molecules, such as antibodies, which are carefully chosen to selectively interact with target receptors on the surface of particular cells. Furthermore, MNPs can be guided to specific sites within the body by applying an external magnetic field, thereby reducing potential side effects. Additionally, the hyperthermic effect elicited by MNPs can be applied in tandem with chemotherapy, thereby increasing the overall treatment efficacy. Considering all of the aforementioned factors, magnetic nanoparticles present as highly promising systems for pharmaceutical delivery and other medical applications. Therefore, thorough evaluations must be carried out to fully understand and leverage their potential.

**Consent for publication:** The authors declared no potential conflicts of interest with respect to the research, authorship, and publication of this article.

**Availability of data and materials:** Not applicable.

**Competing interests:** The authors declare no potential conflicts of interest.

**Funding:** Not applicable.

**Authors' contributions:** Julia Nowak-Jary collected and reviewed literature, wrote an original draft and prepared all the figures. Beata Machnicka participated in the conceptual design and critical revision of the original draft.

**Ethics approval and consent to participate:** Not applicable.

## Abbreviations

**AC** – amino cellulose.

**AC**- alternating current.

 doi:10.20944/preprints202410.0530.v1



**ALP**- alkaline phosphatase.

**ALT**- alkaline aminotransferase.

**AMF**- alternating magnetic field.

**ANT**- adenine nucleotide translocase.

**APTES**- (3-aminopropyl)triethoxysilane.

**APTMS**- (3-aminopropyl)trimethoxysilane.

**BBB**- blood-brain barrier.

**BCECs**- brain capillary endothelial cells.

**BSA** – bovine serum albumin.

**CAT**- catalase.

**CF** – cobalt ferrite.

**CMC**- N-carboxymethyl chitosan.

**CPK-MB**- creatine phosphokinase-MB.

**CS** – chitosan.

**CSF**- cerebrospinal fluid.

**DEAP**- 3-(diethylamino)-propyl amine.

**DEX**- dextran.

**DMSA**- dimercaptosuccinic acid.

**DOX**- doxorubicin.

**EGFR**- epidermal growth factor receptor.

**ETC**- electron transfer chain.

**GGT**- gamma-glutamyl.

**GPx** – glutathione peroxidase.

**GSH**- glutathione reductase.

**HUVECs**- human umbilical vein endothelial cells.

**ICG**- indocyanine green.

**LDH**- lactate dehydrogenase.

**LPS**- lipopolysaccharide.

**MDA**- malondialdehyde.

**MNPs** – magnetic nanoparticles.

**MPTP** – mitochondrial permeability transition pore.

**MRI**- magnetic resonance imaging.

**MTD**- magneto-thermodynamic.

**MTT- 3-(4:5**-dimethylthiazol-2-yl)-2,5-diphenyltetrazolium bromide.

**MTX**- methotrexate.

**NAC**- N-acetylcysteine.

**NSCLC**- non-small cell lung cancer.

**NSCs**- neural stem cells.

**PAA**- polyacrylic acid.

**PAH** – poly(allylamine hydrochloride).

**PAMAM**- polyamidoamine.

 doi:10.20944/preprints202410.0530.v1



**PDADMAC** – poly(diallyl dimethylammonium chloride).

**PEG** – poly(ethylene amine).

**PEI** – poly(ethylene imine).

**PLL**- poly-L-lysine.

**PVA**- polyvinyl alcohol.

**ROS** – reactive oxygen species.

**SOD** – superoxide dismutase.

**TAC**- tacrolimus.

**TEOS**- tetraethoxysilane.

**TLR4**- Toll-like receptor 4.

**VAN**- vancomycin.

**VDAC** – voltage-dependent anion channel.

## References


1. Avval, Z.M.; Malekpour, L.; Raeisi, F.; Babapoor, A.; Mousavi, S.M.; Hashemi, S.A.; Salari, M. Introduction of Magnetic and Supermagnetic Nanoparticles in New Approach of Targeting Drug Delivery and Cancer Therapy Application. *Drug Metabolism Reviews* **2020**, *52*, 157–184, doi:10.1080/03602532.2019.1697282.
2. Estelrich, J.; Escribano, E.; Queralt, J.; Busquets, M. Iron Oxide Nanoparticles for Magnetically-Guided and Magnetically-Responsive Drug Delivery. *Int J Mol Sci* **2015**, *16*, 8070–8101, doi:10.3390/ijms16048070.
3. Foy, S.P.; Manthe, R.L.; Foy, S.T.; Dimitrijevic, S.; Krishnamurthy, N.; Labhasetwar, V. Optical Imaging and Magnetic Field Targeting of Magnetic Nanoparticles in Tumors. *ACS Nano* **2010**, *4*, 5217–5224, doi:10.1021/nn101427t.
4. Stanicki, D.; Vangijzegem, T.; Ternad, I.; Laurent, S. An Update on the Applications and Characteristics of Magnetic Iron Oxide Nanoparticles for Drug Delivery. *Expert Opin Drug Deliv* **2022**, *19*, 321–335, doi:10.1080/17425247.2022.2047020.
5. Palzer, J.; Eckstein, L.; Slabu, I.; Reisen, O.; Neumann, U.P.; Roeth, A.A. Iron Oxide Nanoparticle-Based Hyperthermia as a Treatment Option in Various Gastrointestinal Malignancies. *Nanomaterials* **2021**, *11*, 3013, doi:10.3390/nano11113013.
6. Obaidat, I.M.; Narayanaswamy, V.; Alaabed, S.; Sambasivam, S.; Muralee Gopi, C.V.V. Principles of Magnetic Hyperthermia: A Focus on Using Multifunctional Hybrid Magnetic Nanoparticles. *Magnetochemistry* **2019**, *5*, 67, doi:10.3390/magnetochemistry5040067.
7. Mu, X.; Li, J.; Yan, S.; Zhang, H.; Zhang, W.; Zhang, F.; Jiang, J. siRNA Delivery with Stem Cell Membrane-Coated Magnetic Nanoparticles for Imaging-Guided Photothermal Therapy and Gene Therapy. *ACS Biomater Sci Eng* **2018**, *4*, 3895–3905, doi:10.1021/acsbiomaterials.8b00858.
8. Russell, E.; Dunne, V.; Russell, B.; Mohamud, H.; Ghita, M.; McMahon, S.J.; Butterworth, K.T.; Schettino, G.; McGarry, C.K.; Prise, K.M. Impact of Superparamagnetic Iron Oxide Nanoparticles on in Vitro and in Vivo Radiosensitisation of Cancer Cells. *Radiat Oncol* **2021**, *16*, 104, doi:10.1186/s13014-021-01829-y.
9. De Toledo, L.D.A.S.; Rosseto, H.C.; Bruschi, M.L. Iron Oxide Magnetic Nanoparticles as Antimicrobials for Therapeutics. *Pharm Dev Technol* **2018**, *23*, 316–323, doi:10.1080/10837450.2017.1337793.
10. Rodrigues, G.R.; López-Abarrategui, C.; De La Serna Gómez, I.; Dias, S.C.; Otero-González, A.J.; Franco, O.L. Antimicrobial Magnetic Nanoparticles Based-Therapies for Controlling Infectious Diseases. *Int J Pharm* **2019**, *555*, 356–367, doi:10.1016/j.ijpharm.2018.11.043.
11. Li, Z.; Xue, L.; Wang, P.; Ren, X.; Zhang, Y.; Wang, C.; Sun, J. Biological Scaffolds Assembled with Magnetic Nanoparticles for Bone Tissue Engineering: A Review. *Materials* **2023**, *16*, 1429, doi:10.3390/ma16041429.
12. Skotland, T.; Iversen, T.-G.; Sandvig, K. New Metal-Based Nanoparticles for Intravenous Use: Requirements for Clinical Success with Focus on Medical Imaging. *Nanomedicine* **2010**, *6*, 730–737, doi:10.1016/j.nano.2010.05.002.
13. Wallace, D.F. The Regulation of Iron Absorption and Homeostasis. *Clin Biochem Rev* **2016**, *37*, 51–62.
14. Mai, T.; Hilt, J.Z. Magnetic Nanoparticles: Reactive Oxygen Species Generation and Potential Therapeutic Applications. *J Nanopart Res* **2017**, *19*, 253, doi:10.1007/s11051-017-3943-2.
15. Ahmad, A.; Ansari, Md.M.; Kumar, A.; Vyawahare, A.; Mishra, R.K.; Jayamurugan, G.; Raza, S.S.; Khan, R. Comparative Acute Intravenous Toxicity Study of Triple Polymer-Layered Magnetic Nanoparticles with Bare Magnetic Nanoparticles in Swiss Albino Mice. *Nanotoxicology* **2020**, *14*, 1362–1380, doi:10.1080/17435390.2020.1829144.

16. Mahmoudi, M.; Laurent, S.; Shokrgozar, M.A.; Hosseinkhani, M. Toxicity Evaluations of Superparamagnetic Iron Oxide Nanoparticles: Cell "Vision" *versus* Physicochemical Properties of Nanoparticles. *ACS Nano* **2011**, *5*, 7263–7276, doi:10.1021/nn2021088.
17. Malvindi, M.A.; De Matteis, V.; Galeone, A.; Brunetti, V.; Anyfantis, G.C.; Athanassiou, A.; Cingolani, R.; Pompa, P.P. Toxicity Assessment of Silica Coated Iron Oxide Nanoparticles and Biocompatibility Improvement by Surface Engineering. *PLoS ONE* **2014**, *9*, e85835, doi:10.1371/journal.pone.0085835.
18. Shukla, S.; Jadaun, A.; Arora, V.; Sinha, R.K.; Biyani, N.; Jain, V.K. In Vitro Toxicity Assessment of Chitosan Oligosaccharide Coated Iron Oxide Nanoparticles. *Toxicol Rep* **2015**, *2*, 27–39, doi:10.1016/j.toxrep.2014.11.002.
19. Abakumov, M.A.; Semkina, A.S.; Skorikov, A.S.; Vishnevskiy, D.A.; Ivanova, A.V.; Mironova, E.; Davydova, G.A.; Majouga, A.G.; Chekhonin, V.P. Toxicity of Iron Oxide Nanoparticles: Size and Coating Effects. *J Biochem Mol Toxicol* **2018**, *32*, e22225, doi:10.1002/jbt.22225.
20. Yang, W.; Lee, J.; Hong, S.; Lee, J.; Lee, J.; Han, D.-W. Difference between Toxicities of Iron Oxide Magnetic Nanoparticles with Various Surface-Functional Groups against Human Normal Fibroblasts and Fibrosarcoma Cells. *Materials* **2013**, *6*, 4689–4706, doi:10.3390/ma6104689.
21. Vonarbourg, A.; Passirani, C.; Saulnier, P.; Benoit, J.-P. Parameters Influencing the Stealthiness of Colloidal Drug Delivery Systems. *Biomaterials* **2006**, *27*, 4356–4373, doi:10.1016/j.biomaterials.2006.03.039.
22. Owensiii, D.; Peppas, N. Opsonization, Biodistribution, and Pharmacokinetics of Polymeric Nanoparticles. *Int J Pharm* **2006**, *307*, 93–102, doi:10.1016/j.ijpharm.2005.10.010.
23. Manzanares, D.; Ceña, V. Endocytosis: The Nanoparticle and Submicron Nanocompounds Gateway into the Cell. *Pharmaceutics* **2020**, *12*, 371, doi:10.3390/pharmaceutics12040371.
24. Swanson, J.A.; Baer, S.C. Phagocytosis by Zippers and Triggers. *Trends Cell Biol* **1995**, *5*, 89–93, doi:10.1016/S0962-8924(00)88956-4.
25. Wu, H.; Yin, J.-J.; Wamer, W.G.; Zeng, M.; Lo, Y.M. Reactive Oxygen Species-Related Activities of Nano-Iron Metal and Nano-Iron Oxides. *J Food Drug Anal* **2014**, *22*, 86–94, doi:10.1016/j.jfda.2014.01.007.
26. Sengul, A.B.; Asmatulu, E. Toxicity of Metal and Metal Oxide Nanoparticles: A Review. *Environ Chem Lett* **2020**, *18*, 1659–1683, doi:10.1007/s10311-020-01033-6.
27. Valdiglesias, V.; Kiliç, G.; Costa, C.; Fernández-Bertólez, N.; Pásaro, E.; Teixeira, J.P.; Laffon, B. Effects of Iron Oxide Nanoparticles: Cytotoxicity, Genotoxicity, Developmental Toxicity, and Neurotoxicity: Effects of Iron Oxide Nanoparticles. *Environ Mol Mutagen* **2015**, *56*, 125–148, doi:10.1002/em.21909.
28. Zhang, K. Integration of ER Stress, Oxidative Stress and the Inflammatory Response in Health and Disease. *Int J Clin Exp Med* **2010**, *3*, 33–40.
29. Pongrac, I.M.; Pavičić, I.; Milić, M.; Brkić Ahmed, L.; Babič, M.; Horák, D.; Vinković Vrček, I.; Gajović, S. Oxidative Stress Response in Neural Stem Cells Exposed to Different Superparamagnetic Iron Oxide Nanoparticles. *Int J Nanomedicine* **2016**, *11*, 1701–1715, doi:10.2147/IJN.S102730.
30. Wu, L.; Wen, W.; Wang, X.; Huang, D.; Cao, J.; Qi, X.; Shen, S. Ultrasmall Iron Oxide Nanoparticles Cause Significant Toxicity by Specifically Inducing Acute Oxidative Stress to Multiple Organs. *Part Fibre Toxicol* **2022**, *19*, 24, doi:10.1186/s12989-022-00465-y.
31. Ying, H.; Ruan, Y.; Zeng, Z.; Bai, Y.; Xu, J.; Chen, S. Iron Oxide Nanoparticles Size-Dependently Activate Mouse Primary Macrophages via Oxidative Stress and Endoplasmic Reticulum Stress. *Int Immunopharm* **2022**, *105*, 108533, doi:10.1016/j.intimp.2022.108533.
32. Ansari, M.O.; Parveen, N.; Ahmad, M.F.; Wani, A.L.; Afrin, S.; Rahman, Y.; Jameel, S.; Khan, Y.A.; Siddique, H.R.; Tabish, M.; et al. Evaluation of DNA Interaction, Genotoxicity and Oxidative Stress Induced by Iron Oxide Nanoparticles Both in Vitro and in Vivo: Attenuation by Thymoquinone. *Sci Rep* **2019**, *9*, 6912, doi:10.1038/s41598-019-43188-5.
33. Kenzaoui, B.H.; Bernasconi, C.C.; Hofmann, H.; Juillerat-Jeanneret, L. Evaluation of Uptake and Transport of Ultrasmall Superparamagnetic Iron Oxide Nanoparticles by Human Brain-Derived Endothelial Cells. *Nanomedicine* **2012**, *7*, 39–53, doi:10.2217/nnm.11.85.
34. Zhang, T.; Qian, L.; Tang, M.; Xue, Y.; Kong, L.; Zhang, S.; Pu, Y. Evaluation on Cytotoxicity and Genotoxicity of the L-Glutamic Acid Coated Iron Oxide Nanoparticles. *J Nanosci Nanotechnol* **2012**, *12*, 2866–2873, doi:10.1166/jnn.2012.5763.
35. Du, S.; Li, J.; Du, C.; Huang, Z.; Chen, G.; Yan, W. Overendocytosis of Superparamagnetic Iron Oxide Particles Increases Apoptosis and Triggers Autophagic Cell Death in Human Osteosarcoma Cell under a Spinning Magnetic Field. *Oncotarget* **2017**, *8*, 9410–9424, doi:10.18632/oncotarget.14114.
36. Petters, C.; Thiel, K.; Dringen, R. Lysosomal Iron Liberation Is Responsible for the Vulnerability of Brain Microglial Cells to Iron Oxide Nanoparticles: Comparison with Neurons and Astrocytes. *Nanotoxicology* **2016**, *10*, 332–342, doi:10.3109/17435390.2015.1071445.
37. Hanot, C.C.; Choi, Y.S.; Anani, T.B.; Soundarrajan, D.; David, A.E. Effects of Iron-Oxide Nanoparticle Surface Chemistry on Uptake Kinetics and Cytotoxicity in CHO-K1 Cells. *Int J Mol Sci* **2015**, *17*, 54, doi:10.3390/ijms17010054.

38. Watanabe, M.; Yoneda, M.; Morohashi, A.; Hori, Y.; Okamoto, D.; Sato, A.; Kurioka, D.; Nittami, T.; Hirokawa, Y.; Shiraishi, T.; et al. Effects of $Fe_3O_4$ Magnetic Nanoparticles on A549 Cells. *Int J Mol Sci* **2013**, *14*, 15546–15560, doi:10.3390/ijms140815546.
39. Hohnholt, M.C.; Geppert, M.; Dringen, R. Treatment with Iron Oxide Nanoparticles Induces Ferritin Synthesis but Not Oxidative Stress in Oligodendroglial Cells. *Acta Biomater* **2011**, *7*, 3946–3954, doi:10.1016/j.actbio.2011.06.052.
40. Lindemann, A.; Fraederich, B.M.; Pries, R.; Wollenberg, B.; Lüdtke-Buzug, K.; Graefe, K. Biological Impact of Superparamagnetic Iron Oxide Nanoparticles for Magnetic Particle Imaging of Head and Neck Cancer Cells. *Int J Nanomedicine* **2014**, 5025, doi:10.2147/IJN.S63873.
41. Remya, N.S.; Syama, S.; Sabareeswaran, A.; Mohanan, P.V. Toxicity, Toxicokinetics and Biodistribution of Dextran Stabilized Iron Oxide Nanoparticles for Biomedical Applications. *Int J Pharm* **2016**, *511*, 586–598, doi:10.1016/j.ijpharm.2016.06.119.
42. Repar, N.; Jovičić, E.J.; Kump, A.; Birarda, G.; Vaccari, L.; Erman, A.; Kralj, S.; Nemec, S.; Petan, T.; Drobne, D. Oleic Acid Protects Endothelial Cells from Silica-Coated Superparamagnetic Iron Oxide Nanoparticles (SPIONs)-Induced Oxidative Stress and Cell Death. *Int J Mol Sci* **2022**, *23*, 6972, doi:10.3390/ijms23136972.
43. Ahamed, M.; Alhadlaq, H.A.; Khan, M.A.M.; Akhtar, Mohd.J. Selective Killing of Cancer Cells by Iron Oxide Nanoparticles Mediated through Reactive Oxygen Species via P53 Pathway. *J Nanopart Res* **2013**, *15*, 1225, doi:10.1007/s11051-012-1225-6.
44. Flieger, J.; Franus, W.; Panek, R.; Szymańska-Chargot, M.; Flieger, W.; Flieger, M.; Kołodziej, P. Green Synthesis of Silver Nanoparticles Using Natural Extracts with Proven Antioxidant Activity. *Molecules* **2021**, *26*, 4986, doi:10.3390/molecules26164986.
45. Khalil, I.; Yehye, W.A.; Etxeberria, A.E.; Alhadi, A.A.; Dezfooli, S.M.; Julkapli, N.B.M.; Basirun, W.J.; Seyfoddin, A. Nanoantioxidants: Recent Trends in Antioxidant Delivery Applications. *Antioxidants* **2019**, *9*, 24, doi:10.3390/antiox9010024.
46. Samrot, A.V.; Ram Singh, S.P.; Deenadhayalan, R.; Rajesh, V.V.; Padmanaban, S.; Radhakrishnan, K. Nanoparticles, a Double-Edged Sword with Oxidant as Well as Antioxidant Properties—A Review. *Oxygen* **2022**, *2*, 591–604, doi:10.3390/oxygen2040039.
47. Chavan, R.R.; Bhinge, S.D.; Bhutkar, M.A.; Randive, D.S.; Wadkar, G.H.; Todkar, S.S.; Urade, M.N. Characterization, Antioxidant, Antimicrobial and Cytotoxic Activities of Green Synthesized Silver and Iron Nanoparticles Using Alcoholic Blumea Eriantha DC Plant Extract. *Mater Today Commun* **2020**, *24*, 101320, doi:10.1016/j.mtcomm.2020.101320.
48. Valavanidis, A.; Vlachogianni, T.; Fiotakis, C. 8-Hydroxy-2′ -Deoxyguanosine (8-OHdG): A Critical Biomarker of Oxidative Stress and Carcinogenesis. *J Environ Sci Health C* **2009**, *27*, 120–139, doi:10.1080/10590500902885684.
49. Ayala, A.; Muñoz, M.F.; Argüelles, S. Lipid Peroxidation: Production, Metabolism, and Signaling Mechanisms of Malondialdehyde and 4-Hydroxy-2-Nonenal. *Oxid Med Cell Longev* **2014**, *2014*, 1–31, doi:10.1155/2014/360438.
50. Jahanbani, J.; Ghotbi, M.; Shahsavari, F.; Seydi, E.; Rahimi, S.; Pourahmad, J. Selective Anticancer Activity of Superparamagnetic Iron Oxide Nanoparticles (SPIONs) against Oral Tongue Cancer Using in Vitro Methods: The Key Role of Oxidative Stress on Cancerous Mitochondria. *J Biochem Mol Toxicol* **2020**, *34*, doi:10.1002/jbt.22557.
51. Shi, Y.; Wang, J.; Liu, J.; Lin, G.; Xie, F.; Pang, X.; Pei, Y.; Cheng, Y.; Zhang, Y.; Lin, Z.; et al. Oxidative Stress-Driven DR5 Upregulation Restores TRAIL/Apo2L Sensitivity Induced by Iron Oxide Nanoparticles in Colorectal Cancer. *Biomaterials* **2020**, *233*, 119753, doi:10.1016/j.biomaterials.2019.119753.
52. Dan Dunn, J.; Alvarez, L.A.; Zhang, X.; Soldati, T. Reactive Oxygen Species and Mitochondria: A Nexus of Cellular Homeostasis. *Redox Biology* **2015**, *6*, 472–485, doi:10.1016/j.redox.2015.09.005.
53. Laffon, B.; Fernández-Bertólez, N.; Costa, C.; Brandão, F.; Teixeira, J.P.; Pásaro, E.; Valdiglesias, V. Cellular and Molecular Toxicity of Iron Oxide Nanoparticles. In *Cellular and Molecular Toxicology of Nanoparticles*; Saquib, Q., Faisal, M., Al-Khedhairy, A.A., Alatar, A.A., Eds.; Advances in Experimental Medicine and Biology; Springer International Publishing: Cham, 2018; Vol. 1048, pp. 199–213 ISBN 978-3-319-72040-1.
54. Yarjanli, Z.; Ghaedi, K.; Esmaeili, A.; Rahgozar, S.; Zarrabi, A. Iron Oxide Nanoparticles May Damage to the Neural Tissue through Iron Accumulation, Oxidative Stress, and Protein Aggregation. *BMC Neurosci* **2017**, *18*, 51, doi:10.1186/s12868-017-0369-9.
55. Zhang, Z.; Huang, Q.; Zhao, D.; Lian, F.; Li, X.; Qi, W. The Impact of Oxidative Stress-Induced Mitochondrial Dysfunction on Diabetic Microvascular Complications. *Front Endocrinol (Lausanne)* **2023**, *14*, 1112363, doi:10.3389/fendo.2023.1112363.
56. Guo, C.; Sun, L.; Chen, X.; Zhang, D. Oxidative Stress, Mitochondrial Damage and Neurodegenerative Diseases. *Neural Regen Res* **2013**, *8*, 2003–2014, doi:10.3969/j.issn.1673-5374.2013.21.009.
57. Mancuso, M.; Calsolaro, V.; Orsucci, D.; Carlesi, C.; Choub, A.; Piazza, S.; Siciliano, G. Mitochondria, Cognitive Impairment, and Alzheimer's Disease. *Int J Alzheimer's Dis* **2009**, *2009*, 1–8, doi:10.4061/2009/951548.

58. D'Errico, M.; Parlanti, E.; Pascucci, B.; Filomeni, G.; Mastroberardino, P.G.; Dogliotti, E. The Interplay between Mitochondrial Functionality and Genome Integrity in the Prevention of Human Neurologic Diseases. *Arch Biochem and Biophys* **2021**, *710*, 108977, doi:10.1016/j.abb.2021.108977.
59. Swerdlow, R.H. Mitochondria and Mitochondrial Cascades in Alzheimer's Disease. *J Affect Disord* **2018**, *62*, 1403–1416, doi:10.3233/JAD-170585.
60. Sharma, C.; Kim, S.; Nam, Y.; Jung, U.J.; Kim, S.R. Mitochondrial Dysfunction as a Driver of Cognitive Impairment in Alzheimer's Disease. *Int J Mol Sci* **2021**, *22*, 4850, doi:10.3390/ijms22094850.
61. Shukla, R.K.; Badiye, A.; Vajpayee, K.; Kapoor, N. Genotoxic Potential of Nanoparticles: Structural and Functional Modifications in DNA. *Front Genet* **2021**, *12*, 728250, doi:10.3389/fgene.2021.728250.
62. Bourrinet, P.; Bengele, H.H.; Bonnemain, B.; Dencausse, A.; Idee, J.-M.; Jacobs, P.M.; Lewis, J.M. Preclinical Safety and Pharmacokinetic Profile of Ferumoxtran-10, an Ultrasmall Superparamagnetic Iron Oxide Magnetic Resonance Contrast Agent: *Invest Radiol* **2006**, *41*, 313–324, doi:10.1097/01.rli.0000197669.80475.dd.
63. Zou, J.; Wang, X.; Zhang, L.; Wang, J. Iron Nanoparticles Significantly Affect the *In Vitro* and *In Vivo* Expression of *Id* Genes. *Chem Res Toxicol* **2015**, *28*, 373–383, doi:10.1021/tx500333q.
64. Shahabadi, N.; Akbari, A.; Jamshidbeigi, M.; Falsafi, M. Functionalization of Fe3O4@SiO2 Magnetic Nanoparticles with Nicotinamide and in Vitro DNA Interaction. *J Mol Liq* **2016**, *224*, 227–233, doi:10.1016/j.molliq.2016.09.103.
65. Robinson, J.M. Reactive Oxygen Species in Phagocytic Leukocytes. *Histochem Cell Biol* **2008**, *130*, 281, doi:10.1007/s00418-008-0461-4.
66. Ndozangue-Touriguine, O.; Hamelin, J.; Bréard, J. Cytoskeleton and Apoptosis. *Biochem Pharmacol* **2008**, *76*, 11–18, doi:10.1016/j.bcp.2008.03.016.
67. Askri, D.; Cunin, V.; Béal, D.; Berthier, S.; Chovelon, B.; Arnaud, J.; Rachidi, W.; Sakly, M.; Amara, S.; Sève, M.; et al. Investigating the Toxic Effects Induced by Iron Oxide Nanoparticles on Neuroblastoma Cell Line: An Integrative Study Combining Cytotoxic, Genotoxic and Proteomic Tools. *Nanotoxicology* **2019**, *13*, 1021–1040, doi:10.1080/17435390.2019.1621399.
68. Master, A.M.; Williams, P.N.; Pothayee, N.; Pothayee, N.; Zhang, R.; Vishwasrao, H.M.; Golovin, Y.I.; Riffle, J.S.; Sokolsky, M.; Kabanov, A.V. Remote Actuation of Magnetic Nanoparticles For Cancer Cell Selective Treatment Through Cytoskeletal Disruption. *Sci Rep* **2016**, *6*, 33560, doi:10.1038/srep33560.
69. Connord, V.; Clerc, P.; Hallali, N.; El Hajj Diab, D.; Fourmy, D.; Gigoux, V.; Carrey, J. Real-Time Analysis of Magnetic Hyperthermia Experiments on Living Cells under a Confocal Microscope. *Small* **2015**, *11*, 2437–2445, doi:10.1002/smll.201402669.
70. Zhang, E.; Kircher, M.F.; Koch, M.; Eliasson, L.; Goldberg, S.N.; Renström, E. Dynamic Magnetic Fields Remote-Control Apoptosis *via* Nanoparticle Rotation. *ACS Nano* **2014**, *8*, 3192–3201, doi:10.1021/nn406302j.
71. Shin, E.H.; Li, Y.; Kumar, U.; Sureka, H.V.; Zhang, X.; Payne, C.K. Membrane Potential Mediates the Cellular Binding of Nanoparticles. *Nanoscale* **2013**, *5*, 5879–5886, doi:10.1039/c3nr01667f.
72. Pongrac, I.M.; Dobrivojević, M.; Ahmed, L.B.; Babič, M.; Šlouf, M.; Horák, D.; Gajović, S. Improved Biocompatibility and Efficient Labeling of Neural Stem Cells with Poly(L-Lysine)-Coated Maghemite Nanoparticles. *Beilstein J Nanotechnol* **2016**, *7*, 926–936, doi:10.3762/bjnano.7.84.
73. Gonnissen, D.; Qu, Y.; Langer, K.; Öztürk, C.; Zhao, Y.; Chen, C.; Seebohm, G.; Dufer, M.; Fuchs, H.; Galla, H.-J.; et al. Comparison of Cellular Effects of Starch-Coated SPIONs and Poly(Lactic-Co-Glycolic Acid) Matrix Nanoparticles on Human Monocytes. *Int J Nanomedicine* **2016**, *Volume 11*, 5221–5236, doi:10.2147/IJN.S106540.
74. Yan, L.; Liu, X.; Liu, W.-X.; Tan, X.-Q.; Xiong, F.; Gu, N.; Hao, W.; Gao, X.; Cao, J.-M. $Fe_2O_3$ Nanoparticles Suppress Kv1.3 Channels via Affecting the Redox Activity of Kv $\beta$ 2 Subunit in Jurkat T Cells. *Nanotechnology* **2015**, *26*, 505103, doi:10.1088/0957-4484/26/50/505103.
75. Gualdani, R.; Guerrini, A.; Fantechi, E.; Tadini-Buoninsegni, F.; Moncelli, M.R.; Sangregorio, C. Superparamagnetic Iron Oxide Nanoparticles (SPIONs) Modulate hERG Ion Channel Activity. *Nanotoxicology* **2019**, *13*, 1197–1209, doi:10.1080/17435390.2019.1650969.
76. Shokrollahi, F.; Salehzadeh, A.; Kafilzadeh, F.; Zaefizadeh, M. Evaluation of the Effect of Iron Oxide Nanoparticles Functionalized by Glucose and Conjugated with Coumarin (Fe3O4@Glu-Coumarin NPs) on the Expression of CASP8, CASP9, P53, mTOR1, and MAPK1 Genes in Liver Cancer Cell Line. *Gene Reports* **2023**, *33*, 101818, doi:10.1016/j.genrep.2023.101818.
77. Siddiqui, M.A.; Wahab, R.; Saquib, Q.; Ahmad, J.; Farshori, N.N.; Al-Sheddi, E.S.; Al-Oqail, M.M.; Al-Massarani, S.M.; Al-Khedhairy, A.A. Iron Oxide Nanoparticles Induced Cytotoxicity, Oxidative Stress, Cell Cycle Arrest, and DNA Damage in Human Umbilical Vein Endothelial Cells. *J Trace Elem Med Biol* **2023**, 127302, doi:10.1016/j.jtemb.2023.127302.
78. Hernandes, E.P.; Lazarin-Bidóia, D.; Bini, R.D.; Nakamura, C.V.; Cótica, L.F.; De Oliveira Silva Lautenschlager, S. Doxorubicin-Loaded Iron Oxide Nanoparticles Induce Oxidative Stress and Cell Cycle Arrest in Breast Cancer Cells. *Antioxidants* **2023**, *12*, 237, doi:10.3390/antiox12020237.

79. Rostami, S.; Tafvizi, F.; Kheiri Manjili, H.R. High Efficacy of Tamoxifen-Loaded L-Lysine Coated Magnetic Iron Oxide Nanoparticles in Cell Cycle Arrest and Anti-Cancer Activity for Breast Cancer Therapy. *Bioimpacts* **2022**, *12*, 301–313, doi:10.34172/bi.2021.23337.
80. Majeed, S.; Mohd Rozi, N.A.B.; Danish, M.; Mohamad Ibrahim, M.N.; Joel, E.L. In Vitro Apoptosis and Molecular Response of Engineered Green Iron Oxide Nanoparticles with L-Arginine in MDA-MB-231 Breast Cancer Cells. *J Drug Deliv Sci Technol* **2023**, *80*, 104185, doi:10.1016/j.jddst.2023.104185.
81. Mesárošová, M.; Kozics, K.; Bábelová, A.; Regendová, E.; Pastorek, M.; Vnuková, D.; Buliaková, B.; Rázga, F.; Gábelová, A. The Role of Reactive Oxygen Species in the Genotoxicity of Surface-Modified Magnetite Nanoparticles. *Toxicology Lett* **2014**, *226*, 303–313, doi:10.1016/j.toxlet.2014.02.025.
82. Fernández-Bertólez, N.; Costa, C.; Brandão, F.; Duarte, J.A.; Teixeira, J.P.; Pásaro, E.; Valdiglesias, V.; Laffon, B. Evaluation of Cytotoxicity and Genotoxicity Induced by Oleic Acid-coated Iron Oxide Nanoparticles in Human Astrocytes. *Environ and Mol Mutagen* **2019**, *60*, 816–829, doi:10.1002/em.22323.
83. Riedl, S.J.; Shi, Y. Molecular Mechanisms of Caspase Regulation during Apoptosis. *Nat Rev Mol Cell Biol* **2004**, *5*, 897–907, doi:10.1038/nrm1496.
84. Fridman, J.S.; Lowe, S.W. Control of Apoptosis by P53. *Oncogene* **2003**, *22*, 9030–9040, doi:10.1038/sj.onc.1207116.
85. Grosse, S.; Stenvik, J.; Nilsen, A.M. Iron Oxide Nanoparticles Modulate Lipopolysaccharide-Induced Inflammatory Responses in Primary Human Monocytes. *Int J Nanomedicine* **2016**, *11*, 4625–4642, doi:10.2147/IJN.S113425.
86. Soares, J.-B.; Pimentel-Nunes, P.; Roncon-Albuquerque, R.; Leite-Moreira, A. The Role of Lipopolysaccharide/Toll-like Receptor 4 Signaling in Chronic Liver Diseases. *Hepatol Int* **2010**, *4*, 659–672, doi:10.1007/s12072-010-9219-x.
87. Gerogianni, A.; Bal, M.; Mohlin, C.; Woodruff, T.M.; Lambris, J.D.; Mollnes, T.E.; Sjöström, D.J.; Nilsson, P.H. In Vitro Evaluation of Iron Oxide Nanoparticle-Induced Thromboinflammatory Response Using a Combined Human Whole Blood and Endothelial Cell Model. *Front Immunol* **2023**, *14*, 1101387, doi:10.3389/fimmu.2023.1101387.
88. Chauhan, A.; Anjaly, K.; Saini, A.; Kumar, R.; Kuanr, B.K.; Sharma, D. Vitamin K3-Loaded Magnetic Nanoparticle-Mediated Synergistic Magnetothermodynamic Therapy Evokes Massive ROS and Immune Modulation for Augmented Antitumor Potential. *ACS Appl Mater Interfaces* **2023**, *15*, 27515–27532, doi:10.1021/acsami.3c01702.
89. Cappellini, M.D.; Comin-Colet, J.; De Francisco, A.; Dignass, A.; Doehner, W.; Lam, C.S.; Macdougall, I.C.; Rogler, G.; Camaschella, C.; Kadir, R.; et al. Iron Deficiency across Chronic Inflammatory Conditions: International Expert Opinion on Definition, Diagnosis, and Management. *American J Hematol* **2017**, *92*, 1068–1078, doi:10.1002/ajh.24820.
90. Knutson, M.D. Non-Transferrin-Bound Iron Transporters. *Free Radic Biol Med* **2019**, *133*, 101–111, doi:10.1016/j.freeradbiomed.2018.10.413.
91. Scaramellini, N.; Fischer, D.; Agarvas, A.R.; Motta, I.; Muckenthaler, M.U.; Mertens, C. Interpreting Iron Homeostasis in Congenital and Acquired Disorders. *Pharmaceuticals* **2023**, *16*, 329, doi:10.3390/ph16030329.
92. Chrishtop, V.V.; Mironov, V.A.; Prilepskii, A.Y.; Nikonorova, V.G.; Vinogradov, V.V. Organ-Specific Toxicity of Magnetic Iron Oxide-Based Nanoparticles. *Nanotoxicology* **2021**, *15*, 167–204, doi:10.1080/17435390.2020.1842934.
93. Yang, J.-X.; Tang, W.-L.; Wang, X.-X. Superparamagnetic Iron Oxide Nanoparticles May Affect Endothelial Progenitor Cell Migration Ability and Adhesion Capacity. *Cytotherapy* **2010**, *12*, 251–259, doi:10.3109/14653240903446910.
94. Mulens-Arias, V.; Rojas, J.M.; Sanz-Ortega, L.; Portilla, Y.; Pérez-Yagüe, S.; Barber, D.F. Polyethylenimine-Coated Superparamagnetic Iron Oxide Nanoparticles Impair in Vitro and in Vivo Angiogenesis. *Nanomedicine* **2019**, *21*, 102063, doi:10.1016/j.nano.2019.102063.
95. Cromer Berman, S.M.; Kshitiz; Wang, C.J.; Orukari, I.; Levchenko, A.; Bulte, J.W.M.; Walczak, P. Cell Motility of Neural Stem Cells Is Reduced after SPIO-Labeling, Which Is Mitigated after Exocytosis: Inhibition of Cell Motility and SPIO Exocytosis. *Magn Reson Med* **2013**, *69*, 255–262, doi:10.1002/mrm.24216.
96. Rojas, J.M.; Sanz-Ortega, L.; Mulens-Arias, V.; Gutiérrez, L.; Pérez-Yagüe, S.; Barber, D.F. Superparamagnetic Iron Oxide Nanoparticle Uptake Alters M2 Macrophage Phenotype, Iron Metabolism, Migration and Invasion. *Nanomedicine* **2016**, *12*, 1127–1138, doi:10.1016/j.nano.2015.11.020.
97. Mohsin, A.; Hussain, M.H.; Mohsin, M.Z.; Zaman, W.Q.; Aslam, M.S.; Shan, A.; Dai, Y.; Khan, I.M.; Niazi, S.; Zhuang, Y.; et al. Recent Advances of Magnetic Nanomaterials for Bioimaging, Drug Delivery, and Cell Therapy. *ACS Appl Nano Mater* **2022**, *5*, 10118–10136, doi:10.1021/acsanm.2c02014.
98. Petters, C.; Irrsack, E.; Koch, M.; Dringen, R. Uptake and Metabolism of Iron Oxide Nanoparticles in Brain Cells. *Neurochem Res* **2014**, *39*, 1648–1660, doi:10.1007/s11064-014-1380-5.
99. D'Agata, F.; Ruffinatti, F.; Boschi, S.; Stura, I.; Rainero, I.; Abollino, O.; Cavalli, R.; Guiot, C. Magnetic Nanoparticles in the Central Nervous System: Targeting Principles, Applications and Safety Issues. *Molecules* **2017**, *23*, 9, doi:10.3390/molecules23010009.

100. Thomsen, L.B.; Linemann, T.; Pondman, K.M.; Lichota, J.; Kim, K.S.; Pieters, R.J.; Visser, G.M.; Moos, T. Uptake and Transport of Superparamagnetic Iron Oxide Nanoparticles through Human Brain Capillary Endothelial Cells. *ACS Chem Neurosci* **2013**, *4*, 1352–1360, doi:10.1021/cn400093z.
101. Shin, T.H.; Lee, G. Reduced Lysosomal Activity and Increased Amyloid Beta Accumulation in Silica-Coated Magnetic Nanoparticles-Treated Microglia. *Arch Toxicol* **2024**, *98*, 121–134, doi:10.1007/s00204-023-03612-2.
102. Fahmy, H.M.; Aly, E.M.; Mohamed, F.F.; Noor, N.A.; Elsayed, A.A. Neurotoxicity of Green- Synthesized Magnetic Iron Oxide Nanoparticles in Different Brain Areas of Wistar Rats. *NeuroToxicology* **2020**, *77*, 80–93, doi:10.1016/j.neuro.2019.12.014.
103. Kim, Y.; Kong, S.D.; Chen, L.-H.; Pisanic, T.R.; Jin, S.; Shubayev, V.I. In Vivo Nanoneurotoxicity Screening Using Oxidative Stress and Neuroinflammation Paradigms. *Nanomedicine* **2013**, *9*, 1057–1066, doi:10.1016/j.nano.2013.05.002.
104. Kim, J.S.; Yoon, T.-J.; Yu, K.N.; Kim, B.G.; Park, S.J.; Kim, H.W.; Lee, K.H.; Park, S.B.; Lee, J.-K.; Cho, M.H. Toxicity and Tissue Distribution of Magnetic Nanoparticles in Mice. *Toxicol Sci* **2006**, *89*, 338–347, doi:10.1093/toxsci/kfj027.
105. Ibrahim Fouad, G.; El-Sayed, S.A.M.; Mabrouk, M.; Ahmed, K.A.; Beherei, H.H. Neuroprotective Potential of Intranasally Delivered Sulforaphane-Loaded Iron Oxide Nanoparticles Against Cisplatin-Induced Neurotoxicity. *Neurotox Res* **2022**, *40*, 1479–1498, doi:10.1007/s12640-022-00555-x.
106. Shen, Y.; Gong, S.; Li, J.; Wang, Y.; Zhang, X.; Zheng, H.; Zhang, Q.; You, J.; Huang, Z.; Chen, Y. Co-Loading Antioxidant N-Acetylcysteine Attenuates Cytotoxicity of Iron Oxide Nanoparticles in Hypoxia/Reoxygenation Cardiomyocytes. *Int J Nanomedicine* **2019**, *14*, 6103–6115, doi:10.2147/IJN.S209820.
107. Kumfu, S.; Khamseekaew, J.; Palee, S.; Srichairatanakool, S.; Fucharoen, S.; Chattipakorn, S.C.; Chattipakorn, N. A Combination of an Iron Chelator with an Antioxidant Exerts Greater Efficacy on Cardioprotection than Monotherapy in Iron-Overload Thalassemic Mice. *Free Radic Res* **2018**, *52*, 70–79, doi:10.1080/10715762.2017.1414208.
108. Wongjaikam, S.; Kumfu, S.; Khamseekaew, J.; Sripetchwandee, J.; Srichairatanakool, S.; Fucharoen, S.; Chattipakorn, S.C.; Chattipakorn, N. Combined Iron Chelator and Antioxidant Exerted Greater Efficacy on Cardioprotection Than Monotherapy in Iron-Overloaded Rats. *PLoS ONE* **2016**, *11*, e0159414, doi:10.1371/journal.pone.0159414.
109. Mahmoudi, M.; Hofmann, H.; Rothen-Rutishauser, B.; Petri-Fink, A. Assessing the In Vitro and In Vivo Toxicity of Superparamagnetic Iron Oxide Nanoparticles. *Chem Rev* **2012**, *112*, 2323–2338, doi:10.1021/cr2002596.
110. Iversen, N.K.; Frische, S.; Thomsen, K.; Laustsen, C.; Pedersen, M.; Hansen, P.B.L.; Bie, P.; Fresnais, J.; Berret, J.-F.; Baatrup, E.; et al. Superparamagnetic Iron Oxide Polyacrylic Acid Coated γ-Fe2O3 Nanoparticles Do Not Affect Kidney Function but Cause Acute Effect on the Cardiovascular Function in Healthy Mice. *Toxicol Appl Pharmacol* **2013**, *266*, 276–288, doi:10.1016/j.taap.2012.10.014.
111. Edge, D.; Shortt, C.M.; Gobbo, O.L.; Teughels, S.; Prina-Mello, A.; Volkov, Y.; MacEneaney, P.; Radomski, M.W.; Markos, F. Pharmacokinetics and Bio-Distribution of Novel Super Paramagnetic Iron Oxide Nanoparticles (SPIONs) in the Anaesthetized Pig. *Clin Exp Pharmacol Physiol* **2016**, *43*, 319–326, doi:10.1111/1440-1681.12533.
112. Manickam, V.; Periyasamy, M.; Dhakshinamoorthy, V.; Panneerselvam, L.; Perumal, E. Recurrent Exposure to Ferric Oxide Nanoparticles Alters Myocardial Oxidative Stress, Apoptosis and Necrotic Markers in Male Mice. *Chem-Biol Interact* **2017**, *278*, 54–64, doi:10.1016/j.cbi.2017.10.003.
113. Nemmar, A.; Beegam, S.; Yuvaraju, P.; Yasin, J.; Tariq, S.; Attoub, S.; Ali, B.H. Ultrasmall Superparamagnetic Iron Oxide Nanoparticles Acutely Promote Thrombosis and Cardiac Oxidative Stress and DNA Damage in Mice. *Part Fibre Toxicol* **2015**, *13*, 22, doi:10.1186/s12989-016-0132-x.
114. Shetake, N.G.; Ali, M.; Kumar, A.; Bellare, J.; Pandey, B.N. Theranostic Magnetic Nanoparticles Enhance DNA Damage and Mitigate Doxorubicin-Induced Cardio-Toxicity for Effective Multi-Modal Tumor Therapy. *Biomater Adv* **2022**, *142*, 213147, doi:10.1016/j.bioadv.2022.213147.
115. Ichikawa, Y.; Ghanefar, M.; Bayeva, M.; Wu, R.; Khechaduri, A.; Prasad, S.V.N.; Mutharasan, R.K.; Naik, T.J.; Ardehali, H. Cardiotoxicity of Doxorubicin Is Mediated through Mitochondrial Iron Accumulation. *J Clin Invest* **2014**, *124*, 617–630, doi:10.1172/JCI72931.
116. Jain, D. Cardiotoxicity of Doxorubicin and Other Anthracycline Derivatives. *J Nucl Cardiol* **2000**, *7*, 53–62, doi:10.1067/mnc.2000.103324.
117. Namdari, M.; Eatemadi, A. Cardioprotective Effects of Curcumin-Loaded Magnetic Hydrogel Nanocomposite (Nanocurcumin) against Doxorubicin-Induced Cardiac Toxicity in Rat Cardiomyocyte Cell Lines. *Artif Cells Nanomed Biotechnol* **2017**, *45*, 731–739, doi:10.1080/21691401.2016.1261033.
118. Yang, Y.; Guo, Q.; Peng, J.; Su, J.; Lu, X.; Zhao, Y.; Qian, Z. Doxorubicin-Conjugated Heparin-Coated Superparamagnetic Iron Oxide Nanoparticles for Combined Anticancer Drug Delivery and Magnetic Resonance Imaging. *J Biomed Nanotechnol* **2016**, *12*, 1963–1974, doi:10.1166/jbn.2016.2298.
119. Xiong, F.; Wang, H.; Feng, Y.; Li, Y.; Hua, X.; Pang, X.; Zhang, S.; Song, L.; Zhang, Y.; Gu, N. Cardioprotective Activity of Iron Oxide Nanoparticles. *Sci Rep* **2015**, *5*, 8579, doi:10.1038/srep08579.

120. Nowak-Jary, J.; Machnicka, B. In Vivo Biodistribution and Clearance of Magnetic Iron Oxide Nanoparticles for Medical Applications. *Int J Nanomedicine* **2023**, *Volume 18*, 4067–4100, doi:10.2147/IJN.S415063.
121. Wolf, P.L. Biochemical Diagnosis of Liver Disease. *Indian J Clin Biochem* **1999**, *14*, 59–90, doi:10.1007/BF02869152.
122. Askri, D.; Ouni, S.; Galai, S.; Arnaud, J.; Chovelon, B.; Lehmann, S.G.; Sturm, N.; Sakly, M.; Sève, M.; Amara, S. Intranasal Instillation of Iron Oxide Nanoparticles Induces Inflammation and Perturbation of Trace Elements and Neurotransmitters, but Not Behavioral Impairment in Rats. *Environ Sci Pollut Res* **2018**, *25*, 16922–16932, doi:10.1007/s11356-018-1854-0.
123. Kazemipour, N.; Nazifi, S.; Poor, M.H.H.; Esmailnezhad, Z.; Najafabadi, R.E.; Esmaeili, A. Hepatotoxicity and Nephrotoxicity of Quercetin, Iron Oxide Nanoparticles, and Quercetin Conjugated with Nanoparticles in Rats. *Comp Clin Pathol* **2018**, *27*, 1621–1628, doi:10.1007/s00580-018-2783-5.
124. Salimi, M.; Sarkar, S.; Fathi, S.; Alizadeh, A.; Saber, R.; Moradi, F.; Delavari, H. Biodistribution, Pharmacokinetics, and Toxicity of Dendrimer-Coated Iron Oxide Nanoparticles in BALB/c Mice. *Int J Nanomedicine* **2018**, *13*, 1483–1493, doi:10.2147/IJN.S157293.
125. Yaremenko, A.V.; Zelepukin, I.V.; Ivanov, I.N.; Melikov, R.O.; Pechnikova, N.A.; Dzhalilova, D.Sh.; Mirkasymov, A.B.; Bragina, V.A.; Nikitin, M.P.; Deyev, S.M.; et al. Influence of Magnetic Nanoparticle Biotransformation on Contrasting Efficiency and Iron Metabolism. *J Nanobiotechnol* **2022**, *20*, 535, doi:10.1186/s12951-022-01742-w.
126. Paulini, F.; Marangon, A.R.M.; Azevedo, C.L.; Brito, J.L.M.; Lemos, M.S.; Sousa, M.H.; Veiga-Souza, F.H.; Souza, P.E.N.; Lucci, C.M.; Azevedo, R.B. In Vivo Evaluation of DMSA-Coated Magnetic Nanoparticle Toxicity and Biodistribution in Rats: A Long-Term Follow-Up. *Nanomaterials* **2022**, *12*, 3513, doi:10.3390/nano12193513.
127. Fakhri, Z.; Karimi, N.; Saba, F.; Zhaleh, M. Biocompatibility of Magnetic Nanoparticles Synthesized through Green Routed with a Focus on Hematological and Histological Analysis. *Bioorg Chem* **2023**, *137*, 106552, doi:10.1016/j.bioorg.2023.106552.
128. Rahman, M. Magnetic Resonance Imaging and Iron-Oxide Nanoparticles in the Era of Personalized Medicine. *Nanotheranostics* **2023**, *7*, 424–449, doi:10.7150/ntno.86467.
129. Zhou, K.; Li, Z.-Z.; Cai, Z.-M.; Zhong, N.-N.; Cao, L.-M.; Huo, F.-Y.; Liu, B.; Wu, Q.-J.; Bu, L.-L. Nanotheranostics in Cancer Lymph Node Metastasis: The Long Road Ahead. *Pharmacol Res* **2023**, *198*, 106989, doi:10.1016/j.phrs.2023.106989.
130. Vu-Quang, H.; Yoo, M.-K.; Jeong, H.-J.; Lee, H.-J.; Muthiah, M.; Rhee, J.H.; Lee, J.-H.; Cho, C.-S.; Jeong, Y.Y.; Park, I.-K. Targeted Delivery of Mannan-Coated Superparamagnetic Iron Oxide Nanoparticles to Antigen-Presenting Cells for Magnetic Resonance-Based Diagnosis of Metastatic Lymph Nodes in Vivo. *Acta Biomater* **2011**, *7*, 3935–3945, doi:10.1016/j.actbio.2011.06.044.
131. Sekino, M.; Kuwahata, A.; Ookubo, T.; Shiozawa, M.; Ohashi, K.; Kaneko, M.; Saito, I.; Inoue, Y.; Ohsaki, H.; Takei, H.; et al. Handheld Magnetic Probe with Permanent Magnet and Hall Sensor for Identifying Sentinel Lymph Nodes in Breast Cancer Patients. *Sci Rep* **2018**, *8*, 1195, doi:10.1038/s41598-018-19480-1.
132. Hu, H.; Fu, G.; Ding, Z.; Hu, Y.; Luo, G.; Yin, Z. Polyacrylic Acid-Modified Superparamagnetic Iron Oxide Nanoparticles Differentiate Between Hyperplastic and Metastatic Breast Cancer Lymph Nodes. *J Biomed Nanotechnol* **2023**, *19*, 2085–2092, doi:10.1166/jbn.2023.3721.
133. Kubovcikova, M.; Sobotova, R.; Zavisova, V.; Antal, I.; Khmara, I.; Lisnichuk, M.; Bednarikova, Z.; Jurikova, A.; Strbak, O.; Vojtova, J.; et al. N-Acetylcysteine-Loaded Magnetic Nanoparticles for Magnetic Resonance Imaging. *Int J Mol Sci* **2023**, *24*, 11414, doi:10.3390/ijms241411414.
134. Tenório, M.C.D.S.; Graciliano, N.G.; Moura, F.A.; Oliveira, A.C.M.D.; Goulart, M.O.F. N-Acetylcysteine (NAC): Impacts on Human Health. *Antioxidants* **2021**, *10*, 967, doi:10.3390/antiox10060967.
135. Moacă, E.-A.; Watz, C.; Faur, A.-C.; Lazăr, D.; Socoliuc, V.; Păcurariu, C.; Ianoș, R.; Rus, C.-I.; Minda, D.; Barbu-Tudoran, L.; et al. Biologic Impact of Green Synthetized Magnetic Iron Oxide Nanoparticles on Two Different Lung Tumorigenic Monolayers and a 3D Normal Bronchial Model—EpiAirwayTM Microtissue. *Pharmaceutics* **2022**, *15*, 2, doi:10.3390/pharmaceutics15010002.
136. Sadhukha, T.; Wiedmann, T.S.; Panyam, J. Inhalable Magnetic Nanoparticles for Targeted Hyperthermia in Lung Cancer Therapy. *Biomaterials* **2013**, *34*, 5163–5171, doi:10.1016/j.biomaterials.2013.03.061.
137. Abdelaziz, M.M.; Hefnawy, A.; Anter, A.; Abdellatif, M.M.; Khalil, M.A.F.; Khalil, I.A. Respirable Spray Dried Vancomycin Coated Magnetic Nanoparticles for Localized Lung Delivery. *Int J Pharm* **2022**, *611*, 121318, doi:10.1016/j.ijpharm.2021.121318.
138. Ruiz, A.; Morais, P.C.; Bentes De Azevedo, R.; Lacava, Z.G.M.; Villanueva, A.; Del Puerto Morales, M. Magnetic Nanoparticles Coated with Dimercaptosuccinic Acid: Development, Characterization, and Application in Biomedicine. *J Nanopart Res* **2014**, *16*, 2589, doi:10.1007/s11051-014-2589-6.
139. Chaves, S.B.; Silva, L.P.; Lacava, Z.G.M.; Morais, P.C.; Azevedo, R.B. Interleukin-1 and Interleukin-6 Production in Mice's Lungs Induced by 2, 3 Meso-Dimercaptosuccinic-Coated Magnetic Nanoparticles. *J Appl Phys* **2005**, *97*, 10Q915, doi:10.1063/1.1854531.

140. Zhang, Q.; Yin, R.; Guan, G.; Liu, H.; Song, G. Renal Clearable Magnetic Nanoparticles for Magnetic Resonance Imaging and Guided Therapy. *WIREs Nanomed Nanobiotechnol* **2024**, *16*, e1929, doi:10.1002/wnan.1929.
141. Choi, H.S.; Ipe, B.I.; Misra, P.; Lee, J.H.; Bawendi, M.G.; Frangioni, J.V. Tissue- and Organ-Selective Biodistribution of NIR Fluorescent Quantum Dots. *Nano Lett* **2009**, *9*, 2354–2359, doi:10.1021/nl900872r.
142. Zhou, H.; Ge, J.; Miao, Q.; Zhu, R.; Wen, L.; Zeng, J.; Gao, M. Biodegradable Inorganic Nanoparticles for Cancer Theranostics: Insights into the Degradation Behavior. *Bioconjugate Chem* **2020**, *31*, 315–331, doi:10.1021/acs.bioconjchem.9b00699.
143. Wei, H.; Bruns, O.T.; Kaul, M.G.; Hansen, E.C.; Barch, M.; Wiśniowska, A.; Chen, O.; Chen, Y.; Li, N.; Okada, S.; et al. Exceedingly Small Iron Oxide Nanoparticles as Positive MRI Contrast Agents. *Proc Natl Acad Sci USA* **2017**, *114*, 2325–2330, doi:10.1073/pnas.1620145114.
144. Liu, W.; Deng, G.; Wang, D.; Chen, M.; Zhou, Z.; Yang, H.; Yang, S. Renal-Clearable Zwitterionic Conjugated Hollow Ultrasmall Fe $_3$ O $_4$ Nanoparticles for $T_1$ -Weighted MR Imaging *in Vivo*. *J Mater Chem B* **2020**, *8*, 3087–3091, doi:10.1039/D0TB00086H.
145. Zhou, T.; Dong, Y.; Wang, X.; Liu, R.; Cheng, R.; Pan, J.; Zhang, X.; Sun, S. Highly Sensitive Early Diagnosis of Kidney Damage Using Renal Clearable Zwitterion-Coated Ferrite Nanoprobe via Magnetic Resonance Imaging In Vivo. *Adv Healthcare Materials* **2024**, 2304577, doi:10.1002/adhm.202304577.
146. Al Alalaq, M.A.; Al–Hadedee, L.T.; Alrubeii, A.M.S. Effect of Iron Oxide Nanoparticles Prepared by Chemical Method on the Kidneys, Liver and Brain of Male Mice. *IOP Conf Se.: Earth Environ Sci* **2023**, *1252*, 012132, doi:10.1088/1755-1315/1252/1/012132.
147. Nadia Salem Alrawaiq; Azman Abdullah A Review of Flavonoid Quercetin: Metabolism, Bioactivity and Antioxidant Properties. *Int J PharmTech Res* **2014**, *6*, 933–941.
148. Attia, H.R.; Thalij, K.M. Determination of the Effect of Oral Dosage of Labna Product Supplemented with Fe $_3$ O $_4$ Conjugated with Chitosan Nanoparticles on Growth Parameters, Liver and Kidney Parameters in Anaemic Rats Induced by Phenylhydrazine. *IOP Conf Ser: Earth Environ Sci* **2023**, *1262*, 062049, doi:10.1088/1755-1315/1262/6/062049.
149. Odhiambo, J.F.; DeJarnette, J.M.; Geary, T.W.; Kennedy, C.E.; Suarez, S.S.; Sutovsky, M.; Sutovsky, P. Increased Conception Rates in Beef Cattle Inseminated with Nanopurified Bull Semen1. *Biol Reprod* **2014**, *91*, doi:10.1095/biolreprod.114.121897.
150. Feugang, J.M.; Rhoads, C.E.; Mustapha, P.A.; Tardif, S.; Parrish, J.J.; Willard, S.T.; Ryan, P.L. Treatment of Boar Sperm with Nanoparticles for Improved Fertility. *Theriogenology* **2019**, *137*, 75–81, doi:10.1016/j.theriogenology.2019.05.040.
151. Rateb, S.A. Purification of Cryopreserved Camel Spermatozoa Following Protease-based Semen Liquefaction by Lectin-functionalized DNA-defrag Magnetic Nanoparticles. *Reprod Domestic Animals* **2021**, *56*, 183–192, doi:10.1111/rda.13863.
152. Kim, J.H.; Lee, H.J.; Doo, S.H.; Yang, W.J.; Choi, D.; Kim, J.H.; Won, J.H.; Song, Y.S. Use of Nanoparticles to Monitor Human Mesenchymal Stem Cells Transplanted into Penile Cavernosum of Rats with Erectile Dysfunction. *Korean J Urol* **2015**, *56*, 280, doi:10.4111/kju.2015.56.4.280.
153. Sundarraj, K.; Manickam, V.; Raghunath, A.; Periyasamy, M.; Viswanathan, M.P.; Perumal, E. Repeated Exposure to Iron Oxide Nanoparticles Causes Testicular Toxicity in Mice. *Environ Toxicol* **2017**, *32*, 594–608, doi:10.1002/tox.22262.
154. Noori A; Parivar K; Modaresi M; Messripour M; Yousefi MH; Amiri GR Effect of Magnetic Iron Oxide Nanoparticles on Pregnancy and Testicular Development of Mice. *Afr J Biotechnol* **2011**, *10*, 1221–1227, doi:10.5897/AJB10.1544.
155. Al-Shammari, M.S.; Al-Saaidi, J.A. Influence of Magnetic Iron Oxide Nanoparticles in Reproductive Efficiency of Adult Male Rats. *Int J Vet Sci* **2023**, *37*, 507–513, doi:10.33899/ijvs.2022.133978.2326.
156. Zhao, Y.; Ng, K.W. Nanotoxicology in the Skin: How Deep Is the Issue? *Nano LIFE* **2014**, *04*, 1440004, doi:10.1142/S1793984414400042.
157. Silva, S.A.M.E.; Michniak-Kohn, B.; Leonardi, G.R. An Overview about Oxidation in Clinical Practice of Skin Aging. *An Bras Dermatol* **2017**, *92*, 367–374, doi:10.1590/abd1806-4841.20175481.
158. Amin, R.M.; Abdelmonem, A.; Verwanger, T.; Elsherbini, E.; Krammer, B. Cytotoxicity of Magnetic Nanoparticles on Normal and Malignant Human Skin Cells. *Nano LIFE* **2014**, *04*, 1440002, doi:10.1142/S1793984414400029.
159. Duval, K.E.A.; Vernice, N.A.; Wagner, R.J.; Fiering, S.N.; Petryk, J.D.; Lowry, G.J.; Tau, S.S.; Yin, J.; Houde, G.R.; Chaudhry, A.S.; et al. Immunogenetic Effects of Low Dose (CEM43 30) Magnetic Nanoparticle Hyperthermia and Radiation in Melanoma Cells. *Int J Hyperther* **2019**, *36*, 37–46, doi:10.1080/02656736.2019.1627433.
160. Amatya, R.; Kim, D.; Min, K.A.; Shin, M.C. Iron Oxide Nanoparticles-Loaded Hydrogels for Effective Topical Photothermal Treatment of Skin Cancer. *J Pharm Investig* **2022**, *52*, 775–785, doi:10.1007/s40005-022-00593-9.

161. Buchman, J.T.; Hudson-Smith, N.V.; Landy, K.M.; Haynes, C.L. Understanding Nanoparticle Toxicity Mechanisms To Inform Redesign Strategies To Reduce Environmental Impact. *Ac. Chem Res* **2019**, *52*, 1632–1642, doi:10.1021/acs.accounts.9b00053.
162. Nowak-Jary J, Płóciennik A, Machnicka B. Functionalized Magnetic Fe3O4 Nanoparticles for Targeted Methotrexate Delivery in Ovarian Cancer Therapy. *Int J Mol Sc*i **2024**, *25*, 9098, doi:10.3390/ijms25169098.
163. Misra, S.K.; Dybowska, A.; Berhanu, D.; Luoma, S.N.; Valsami-Jones, E. The Complexity of Nanoparticle Dissolution and Its Importance in Nanotoxicological Studies. *Sci Total Environ* **2012**, *438*, 225–232, doi:10.1016/j.scitotenv.2012.08.066.
164. Ucar, A.; Parlak, V.; Ozgeris, F.B.; Yeltekin, A.C.; Arslan, M.E.; Alak, G.; Turkez, H.; Kocaman, E.M.; Atamanalp, M. Magnetic Nanoparticles-Induced Neurotoxicity and Oxidative Stress in Brain of Rainbow Trout: Mitigation by Ulexite through Modulation of Antioxidant, Anti-Inflammatory, and Antiapoptotic Activities. *Sci Total Environ* **2022**, *838*, 155718, doi:10.1016/j.scitotenv.2022.155718.
165. Bardestani, A.; Ebrahimpour, S.; Esmaeili, A.; Esmaeili, A. Quercetin Attenuates Neurotoxicity Induced by Iron Oxide Nanoparticles. *J Nanobiotechnol* **2021**, *19*, 327, doi:10.1186/s12951-021-01059-0.
166. Durdík, Š.; Vrbovská, H.; Olas, A.; Babincová, M. Influence of Naturally Occurring Antioxidants on Magnetic Nanoparticles: Risks, Benefits, and Possible Therapeutic Applications. *Gen Physiol Biophys* **2013**, *32*, 173–177, doi:10.4149/gpb_2013039.
167. Chen, L.; Wu, L.; Liu, F.; Qi, X.; Ge, Y.; Shen, S. Azo-Functionalized Fe $_3$ O $_4$ Nanoparticles: A near-infrared Light Triggered Drug Delivery System for Combined Therapy of Cancer with Low Toxicity. *J Mater Chem B* **2016**, *4*, 3660–3669, doi:10.1039/C5TB02704G.
168. Hohnholt, M.C.; Dringen, R. Iron-Dependent Formation of Reactive Oxygen Species and Glutathione Depletion after Accumulation of Magnetic Iron Oxide Nanoparticles by Oligodendroglial Cells. *J Nanopart Res* **2011**, 13, 6761–6774, doi:10.1007/s11051-011-0585-7.
169. Yang.; Kuang, H.; Zhang, W.; Aguilar, Z.P.; Xiong, Y.; Lai, W.; Xu, H.; Wei, H. Size Dependent Biodistribution and Toxicokinetics of Iron Oxide Magnetic Nanoparticles in Mice. *Nanoscale* **2015**, *7*, 625–636, doi:10.1039/C4NR05061D.
170. Wang, Q.; Shen, M.; Zhao, T.; Xu, Y.; Lin, J.; Duan, Y.; Gu, H. Low Toxicity and Long Circulation Time of Polyampholyte-Coated Magnetic Nanoparticles for Blood Pool Contrast Agents. *Sci Rep* **2015**, *5*, 7774, doi: 10.1038/srep07774.
171. Agotegaray, M.; Campelo, A.; Zysler, R.; Gumilar, F.; Bras, C.; Minetti, A.; Massheimer, V.; Lassalle, V. Influence of Chitosan Coating on Magnetic Nanoparticles in Endothelial Cells and Acute Tissue Biodistribution. *J Biomater Sci Polym Ed* **2016**, *27*, 1069–1085, doi: 10.1080/09205063.2016.1170417.
172. Bhandari, R.; Gupta, P.; Dziubla, T.; Hilt, J.Z. Single Step Synthesis, Characterization and Applications of Curcumin Functionalized Iron Oxide Magnetic Nanoparticles. *Mater Sci Eng C Mater Biol Appl* **2016**, *67*, 59-64, doi: 10.1016/j.msec.2016.04.093.
173. Iacovita, C.; Florea, A.; Dudric, R.; Pall, E.; Moldovan, A.; Tetean, R.; Stiufiuc, R.; Lucaciu, C. Small versus Large Iron Oxide Magnetic Nanoparticles: Hyperthermia and Cell Uptake Properties. *Molecules* **2016**, *21*, 1357, doi: 10.3390/molecules21101357.
174. Jarockyte, G.; Dangelaite, E.; Stasys, M.; Statkute, U.; Poderys, V.; Tseng, T.-C.; Hsu, S.-H.; Karabanovas, V.; Rotomskis, R. Accumulation and Toxicity of Superparamagnetic Iron Oxide Nanoparticles in Cells and Experimental Animals. *Int J Mol Sci* **2016**, *17*, 1193, doi: 10.3390/ijms17081193.
175. Zhang, L.; Wang, X.; Miao, Y.; Chen, Z.; Qiang, P.; Cui, L.; Jing, H.; Guo, Y. Magnetic Ferroferric Oxide Nanoparticles Induce Vascular Endothelial Cell Dysfunction and Inflammation by Disturbing Autophagy. *J Hazard Mater* **2016**, *304*, 186–195, doi: 10.1016/j.jhazmat.2015.10.041.
176. Agotegaray, M.A.; Campelo, A.E.; Zysler, R.D.; Gumilar, F.; Bras, C.; Gandini, A.; Minetti, A.; Massheimer, V.L.; Lassalle, V.L. Magnetic Nanoparticles for Drug Targeting: From Design to Insights into Systemic Toxicity. Preclinical Evaluation of Hematological, Vascular and Neurobehavioral Toxicology. *Biomater Sci* **2017**, *5*, 772–783, doi: 10.1039/C6BM00954A.
177. Feng, Q.; Liu, Y.; Huang, J.; Chen, K.; Huang, J.; Xiao, K. Uptake, Distribution, Clearance, and Toxicity of Iron Oxide Nanoparticles with Different Sizes and Coatings. *Sci Rep* **2018**, *8*, 2082, doi: 10.1038/s41598-018-19628-z.
178. Marimon-Bolívar, W.; Tejeda-Benítez, L.P.; Núñez-Avilés, C.A.; De Léon-Pérez, D.D. Evaluation of the in Vivo Toxicity of Green Magnetic Nanoparticles Using Caenorhabditis Elegans as a Biological Model. E*nviron Nanotechnol Monit Manag* **2019**, *12*, 100253, doi: 10.1016/j.enmm.2019.100253.
179. Ayubi, M.; Karimi, M.; Abdpour, S.; Rostamizadeh, K.; Parsa, M.; Zamani, M.; Saedi, A. Magnetic Nanoparticles Decorated with PEGylated Curcumin as Dual Targeted Drug Delivery: Synthesis, Toxicity and Biocompatibility Study. *Mater Sci Eng C* **2019**, *104*, 109810, doi: 10.1016/j.msec.2019.109810.
180. Patsula, V.; Tulinska, J.; Trachtová, Š.; Kuricova, M.; Liskova, A.; Španová, A.; Ciampor, F.; Vavra, I.; Rittich Ursinyova, M.; Dusinska, M.; Ilavska, S.; Horvathova, M.; Masanova, V.; Uhnakova, I.; Horák, D. Toxicity Evaluation of Monodisperse PEGylated Magnetic Nanoparticles for Nanomedicine. *Nanotoxicology* **2019**, *13*, 510–526, doi: 10.1080/17435390.2018.1555624.

181. Caro, C.; Egea-Benavente, D.; Polvillo, R.; Royo, J.L.; Pernia Leal, M.; García-Martín, M.L. Comprehensive Toxicity Assessment of PEGylated Magnetic Nanoparticles for in Vivo Applications. *Colloid Surface B* **2019**,*177*, 253–259, doi: 10.1016/j.colsurfb.2019.01.051.
182. Nosrati, H.; Salehiabar, M.; Fridoni, M.; Abdollahifar, M.-A.; Kheiri Manjili, H.; Davaran, S.; Danafar, H. New Insight about Biocompatibility and Biodegradability of Iron Oxide Magnetic Nanoparticles: Stereological and In Vivo MRI Monitor. *Sci Rep* **2019,** *9*, 7173, doi: 10.1038/s41598-019-43650-4.
183. Farid, R.M.; Gaafar, P.M.E.; Hazzah, H.A.; Helmy, M.W.; Abdallah, O.Y. Chemotherapeutic Potential of L-Carnosine from Stimuli-Responsive Magnetic Nanoparticles against Breast Cancer Model. *Nanomedicine* **2020**, *15*, 891–911, doi: 10.2217/nnm-2019-0428.
184. Rozhina, E.; Danilushkina, A.; Akhatova, F.; Fakhrullin, R.; Rozhin, A.; Batasheva, S. Biocompatibility of Magnetic Nanoparticles Coating with Polycations Using A549 Cells. *J Biotechnology* **2021**, *325*, 25–34, doi: 10.1016/j.jbiotec.2020.12.003.
185. Chandekar, K.V.; Shkir Mohd Alshahrani, T.; Ibrahim, E.H.; Kilany, M.; Ahmad, Z.; Manthrammel, M.A.; Al Faify, S.; Kateb, B.; Kaushik, A. One-Spot Fabrication and in-Vivo Toxicity Evaluation of Core-Shell Magnetic Nanoparticles. *Mater Sci Eng C* **2021**, *122*, 111898, doi: 10.1016/j.msec.2021.111898.
186. Qi, J.; Zhang, J.; Jia, H.; Guo, X.; Yue, Y.; Yuan, Y.; Yue, T. Synthesis of Silver/Fe3O4@chitosan@polyvinyl Alcohol Magnetic Nanoparticles as an Antibacterial Agent for Accelerating Wound Healing. *Int J Biol Macromol* **2022**, *221*, 1404–1414, doi: 10.1016/j.ijbiomac.2022.09.030.
187. Obireddy, S.R.; Lai, W.-F. ROS-Generating Amine-Functionalized Magnetic Nanoparticles Coupled with Carboxymethyl Chitosan for pH-Responsive Release of Doxorubicin. *Int J Nanomedicine* **2022**, *17*, 589–601, doi: 10.2147/IJN.S338897.
188. Jiang, Y.; Xu, X.; Lu, J.; Yin, C.; Li, G.; Bai, L.; Zhang, T.; Mo, J.; Wang, X.; Shi, Q.; Wang, T.; Zhou, Q. Development of ε-Poly(L-Lysine) Carbon Dots-Modified Magnetic Nanoparticles and Their Applications as Novel Antibacterial Agents. *Front Chem* **2023**, *11*, 1184592, doi: 10.3389/fchem.2023.1184592.
189. Do, X.-H.; Nguyen, T.D.; Le, T.T.H.; To, T.T.; Bui, T.V.K.; Pham, N.H.; Lam, K.; Hoang, T.M.N.; Ha, P.T. High Biocompatibility, MRI Enhancement, and Dual Chemo- and Thermal-Therapy of Curcumin-Encapsulated Alginate/$Fe_3O_4$ Nanoparticles. *Pharmaceutics* **2023**, *15*, 1523, doi:10.3390/pharmaceutics15051523.